Information). As shown in the figure, the tradeoff between the $p_{accurate}$ and $p_{compress}$ values obtained by the vote-by-percent strategy was the worst of all the vote-by approaches. For the vote-by-number and vote-by-rank strategies, smaller $x_{threshold}$ and $y_{threshold}$ values gave smaller (better) compression ratios when similar $p_{accurate}$ values were obtained. For example, if $p_{accurate} \geq 0.9$ was required, the best $p_{compress}$ for the vote-by-rank was around 2.6% and was obtained using $y_{threshold} = 1$ and $w_{threshold} = 1$. These thresholds mean that each scoring function votes for only the top model, and the models that win one or more votes are selected. The same results can be obtained using the vote-by-number strategy when the $x_{threshold}$ is small enough, because the autoscaled score value of the top model is always 0. The compression ratio produced by this threshold was the best of all the consensus scores, including not only the vote-by but also the number-by, rank-by, and percent-by strategies for the condition of $p_{accurate} \geq 0.9$. By contrast, it is difficult to adjust the parameters for vote-by strategies because of the requirement for two thresholds; thus, other strategies, such as the rank-by-number approach, might be more suitable for easy-to-use consensus scoring.

**3.4. Consensus Scores for Complexes with High Binding Affinities.** Sections 3.1−3.3 discussed our investigations of all 220 protein−ligand complex systems. The current section describes the analysis of the 57 complexes with high affinities that are marked in bold in Table S1 of the Supporting Information.

Figure S4 in the Supporting Information shows the compression ratios produced by the nine consensus scoring strategies under the condition that gave reasonable models for all 57 systems without exception (that is, $p_{accurate} = 1.0$). The results that were obtained using the best combinations, all nine functions, and five CScore functions are illustrated. The number-by-number and vote-by-number strategies were appropriate for the 57 complexes, which was consistent with the results obtained for all 220 test complexes. These findings suggest that the results for the 220 complexes will also be useful for designing high-affinity ligands, which could play important roles in drug design trials.

In addition to the calculations under the condition $p_{accurate} = 1.0$, the tradeoffs between the $p_{accurate}$ and $p_{compress}$ values were investigated for the 57 complexes with high-affinity ligands using several threshold values. The results are shown in Figure 8. The balances between the $p_{accurate}$ and $p_{compress}$ values obtained using the best combinations for number-by, rank-by, and percent-by strategies are shown in Figure 8a (similar to those presented in Figure 5). Figure 8b, which corresponds to Figure 7b, illustrates the tradeoffs between the $p_{accurate}$ and $p_{compress}$ values for the vote-by-rank strategy using all nine functions. According to these calculations, the results of the rank-by and percent-by strategies were better than those of the number-by strategies. For the vote-by-rank, $y_{threshold} = 1$ was the best voting standard threshold. These findings were consistent with the earlier discussions of all 220 complexes.

**3.5. Consensus Scores for Experimental Complex Structures.** In this section, we discuss the abilities of consensus scores for use with experimentally observed complex structures. Calculating the consensus score values for various experimental structures (that is, the "correct answer") revealed how small scores could be obtained for

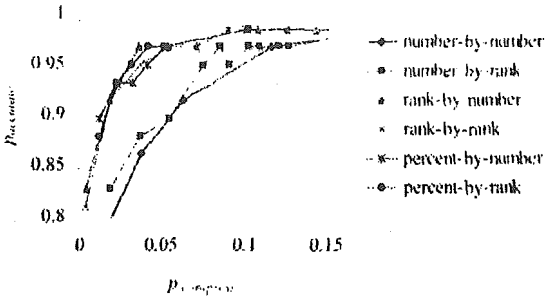


(a) Number-by-, rank-by- and percent-by- strategies.

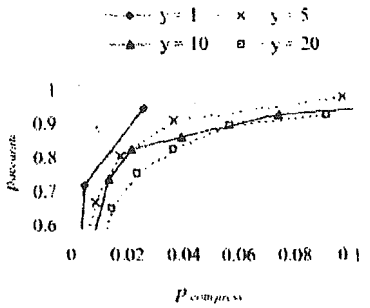


(b) Vote-by-rank strategies (using all nine functions).

**Figure 8.** Compression ratios versus the ratios of accurate modeling for the test set including complexes with high-affinity ligands.

**Table 4.** Thresholds of Number-by-Number Consensus Scores for the Experimental Complex Structures

| | $x_{threshold}$ | |
|---|---|---|
| | all complexes | complexes with high-affinity ligands |
| best combination | 0.386 | 0.271 |
| using all nine functions | 0.689 | 0.513 |
| using the five CScore functions | 0.785 | 0.676 |

compounds that experimentally docked into target proteins. In this study, the number-by-number strategy was used for this purpose.

Table 4 and Figure 9 present the computational results for the experimental structures produced using the number-by-number strategy. The thresholds under which reasonable models can be selected (that is, the worst value for the number-by-number strategy) are described for all 220 experimental structures and for the 57 complexes with high-affinity ligands. The score value for the test set including complexes with high-affinity ligands was better than that for the whole test set. This suggests that, when the ligand with a better score is selected, a higher binding affinity can be expected using the number-by-number strategy. In addition, the frequency distributions of the consensus score values of the experimental structures are illustrated in Figure 9. For practical reasons, we used the combinations including all nine scoring functions and the five CScore functions. For the high-affinity ligands, the number-by-number values were less than 0.3 for 90% of the 57 experimental structures produced using all nine functions.

**3.6. Consensus Scores for Complexes with More Than or Equal to 250 Candidates Generated by Computational**

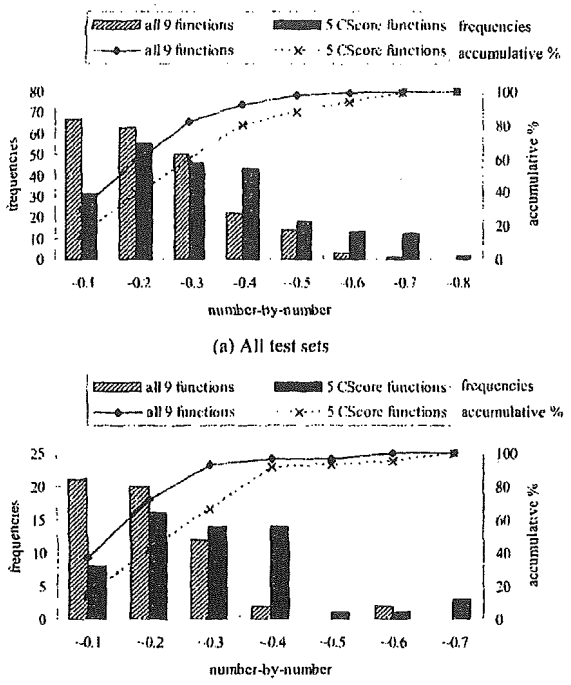


**Figure 9.** Frequency distributions and accumulative percentages of number-by-number values for the experimental complex structures.

**Docking.** In computational docking, the numbers of generated candidates depend on flexibilities of ligands and sizes of active sites of target proteins. As shown in Table S1 of the Supporting Information, in this study, the number of candidates was between 6 and 500. To find the consensus scoring strategies which can be widely used, various types of test complexes, for which various numbers of candidates were generated, need to be investigated as mentioned in Sections 3.1−3.5. However, the large differences of the numbers of candidates possibly cause bias for the ranks and percentages. In this section, the comparisons of consensus scores for only 122 test complexes which have more than or equal to 250 model candidates generated by FlexX were carried out in order to reduce the bias.

Figure 10 shows a comparison of the $p_{compress}$ values of the nine consensus scoring strategies under the condition $p_{accurate} = 1.0$. As shown in this figure, the results of the best combinations of percent-by strategies were as good as or better than those of vote-by-number and number-by-number for complexes with $n \geq 250$ although both percent-by strategies gave much worse $p_{compress}$ values than vote-by-number and number-by-number in a test for all 220 complexes, as mentioned in Section 3.1. On the other hand, for the combinations including all nine functions and five CScore functions, results of the percent-by strategies were worse than those of vote-by-number and number-by-number. It indicates that vote-by-number and number-by-number are more appropriate in terms of the robustness of combinations of scoring functions not only for complete test sets but also for complexes with $n \geq 250$. For rank-by-number and vote-by-rank, although $p_{compress}$ values were highly improved in comparison with the results shown in Table 2 in Section 3.1, they remain worse than those of vote-by-number and number-by-number. These results suggest that although ranks and percentages are affected by the number of model candidates ($n$), vote-by-number and number-by-number are still appropriate under the condition $p_{accurate} = 1.0$ because they workwell regardless of whether $n$ is large or not and they are robust in terms of combinations of scoring functions.

In Figure 11, the tradeoffs between $p_{accurate}$ and $p_{compress}$

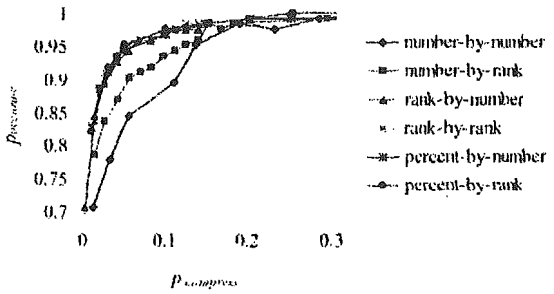


**Figure 11.** Compression ratios versus the ratios of accurate modeling for the test set including complexes with $n \geq 250$.

for complexes with $n \geq 250$ are illustrated. As shown in this figure, the results were similar to those in Figure 5 in Section 3.2. Thus, to achieve a good balance between $p_{accurate}$ and $p_{compress}$, rank-by and percent-by strategies were appropriate regardless of the number of candidates. Both the results of studies with conditions under $p_{accurate} = 1.0$ and those of tradeoff studies for complexes with $n \geq 250$ were consistent with those for all 220 complexes, and they indicate that the results of this study are useful for various systems regardless of the numbers of generated candidates within the limitation of "Num.Answers" = 500.

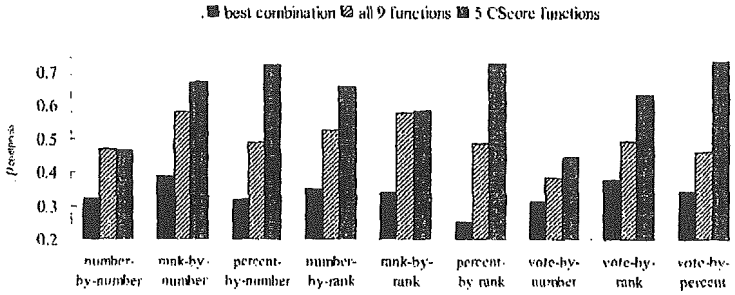


**Figure 10.** Compression ratios for the focused test set including complexes with $n \geq 250$.

## 4. CONCLUSIONS

In this study, we investigated the abilities of consensus scores to evaluate docking models constructed using FlexX. We systematically named the nine types of consensus scoring strategies that have been independently proposed (and previously confused with one another) and compared their performance. All 511 types of combinations including the nine scoring functions were investigated for each of the strategies. Consequently, we found that the number-by-number and vote-by-number strategies were appropriate for use in model selection in all of the systems without exception, and the rank-by-number and percent-by-number strategies were useful for model selection with a good tradeoff between accuracy and efficiency. Considering the scoring functions that were utilized, PLP and DrugScore, which were effective for model selection in single scoring systems, were also appropriate for use in consensus scores. In addition, GOLD score and DOCK score, which were not effective in single scoring systems, were also useful in consensus scoring approaches, as they seemed to compensate for the shortcomings of the other scoring functions. Optimizing the combinations of scoring functions is expensive in terms of computational costs, so consensus scores including all nine functions or the five CScore functions without the need for prior optimizations are particularly useful in practice. Although the vote-by strategies were effective for model selection, they require two types of threshold to be defined, and it is difficult to control the numbers of finally selected models. Thus, we recommend the number-by-number strategy (for all systems without exception) or the rank-by-number strategy (for a good balance between accuracy and efficiency), both of which have abilities similar to those of the vote-by strategies.

In previous papers,[17-20,31,32] the vote-by-percent strategy has been used as a representative of vote-by approaches (denoted as rank-by-vote in refs 17 and 20, and the "intersection approach" in ref 31) for compound selection in virtual screening trials. Some of these studies reported that vote-by strategies did not work well in comparison to other approaches or single scoring.[17,19,31] However, as shown in the current study, the vote-by-percent approach is the least appropriate of all the vote-by strategies, at least for model selection, and other techniques should be used for discussions of the abilities of vote-by strategies. Although the scoring scheme of compound selection in virtual screening is different from that of model selection in computational docking, the vote-by-percent strategy might not be appropriate for virtual screening, as is the case in model selections. In our study, the abilities of consensus scores were discussed only for use in model selection in computational docking, and we intend to systematically investigate the performance of consensus scores in virtual screening in future trials.

In the current study, model selection for all systems without exception, and for most systems with few exceptions, were investigated. This is the first comparison of the use of consensus scores in these two situations, and we found that different types of strategies are required. If vote-by strategies are inadequate because of practical problems, number-by-number and rank-by-number approaches should be suitable for the former and latter situations, respectively. We previously described the by-number-type consensus score AASS[30] and argued that both the number-by-AASS and rank-by-AASS approaches should be used according to the demands of the specific situation.

Although this study focused on the selection of docking models produced by FlexX, we expect our results to be relevant to other computational docking programs. We intend to investigate these aspects further in a future study.

**Supporting Information Available:** Lists of the protein–ligand complexes for the test set, top 10 combinations of the scores, dependencies of $p_{accurate}$ and $p_{compress}$ on $w_{threshold}$, the figures of dependencies of $p_{accurate}$ on threshold, and the figures of $p_{compress}$ under the condition $p_{accurate} = 1.0$. This material is available free of charge via the Internet at http://pubs.acs.org.

## REFERENCES AND NOTES


(1) Kroemer, R. T. Molecular Modelling Probes: Docking and Scoring. *Biochem. Soc. Trans.* **2003**, *31*, 980–984.
(2) Leach, A. R. In *Molecular Modelling*, 2nd ed.; Pearson Education Limited: Essex, 2001; Chapter 12, pp 640–726.
(3) Kitchen, D. B.; Decornez, H.; Furr, J. R.; Bajorath, J. Docking and Scoring in Virtual Screening for Drug Discovery: Methods and Applications, *Nat. Rev. Drug Discovery* **2004**, *3*, 935–949.
(4) Rarey, M.; Kramer, B.; Lengauer, T.; Klebe, G. A Fast Flexible Docking Method Using an Incremental Construction Algorithm. *J. Mol. Biol.* **1996**, *261*, 470–489.
(5) Jones, G.; Willett, P.; Glen, R. C.; Leach, A. R.; Taylor, R. Development and Validation of a Genetic Algorithm for Flexible Docking. *J. Mol. Biol.* **1997**, *267*, 727–748.
(6) Kuntz, I. D.; Blaney, J. M.; Oatley, S. J.; Langridge, R.; Ferrin, T. E. A Geometric Approach to Macromolecule–Ligand Interactions. *J. Mol. Biol.* **1982**, *161*, 269–288.
(7) Friesner, R. A.; Banks, J. L.; Murphy, R. B.; Halgren, T. A.; Klicic, J. J.; Mainz, D. T.; Repasky, M. P.; Knoll, E. H.; Shelley, M.; Perry, J. K.; Shaw, D. E.; Francis, P.; Shenkin, P. S. Glide: A New Approach for Rapid, Accurate Docking and Scoring. 1. Method and Assessment of Docking Accuracy. *J. Med. Chem.* **2004**, *47*, 1739–1749.
(8) Muegge, I.; Martin, Y. C. A General and Fast Scoring Function for Protein–Ligand Interactions: A Simplified Potential Approach. *J. Med. Chem.* **1999**, *42*, 791–804.
(9) Eldridge, M. D.; Murray, C. W.; Auton, T. R.; Paolini, G. V.; Mee, R. P. Empirical Scoring Functions: I. The Development of a Fast Empirical Scoring Function to Estimate the Binding Affinity of Ligand in Receptor Complexes. *J. Comput.-Aided Mol. Des.* **1997**, *11*, 425–445.
(10) Murray, C. W.; Auton, T. R.; Eldridge, M. D. Empirical Scoring Functions. II. The Testing of an Empirical Scoring Function for the Prediction of Ligand–Receptor Binding Affinities and the Use of Bayesian Regression to Improve the Quality of the Model. *J. Comput.-Aided Mol. Des.* **1998**, *12*, 503–519.
(11) Gohlke, H.; Hendlich, M.; Klebe, G. Knowledge-based Scoring Function to Predict Protein–Ligand Interactions. *J. Mol. Biol.* **2000**, *295*, 337–356.
(12) Gehlhaar, D. K.; Verkhivker, G. M.; Rejto, P. A.; Sherman, C. J.; Fogel, D. B.; Fogel, L. J.; Freer, S. T. Molecular Recognition of the Inhibitor AG-1343 by HIV-1 Protease: Conformationally Flexible Docking by Evolutionary Programming. *Chem. Biol.* **1995**, *2*, 317–324.
(13) Wang, R.; Lai, L.; Wang, S. Further Development and Validation of Empirical Scoring Functions for Structure-Based Binding Affinity Prediction. *J. Comput.-Aided Mol. Des.* **2002**, *16*, 11–26.
(14) Stahl, M.; Schulz-Gasch, T. Practical Database Screening with Docking Tools. *Ernst Schering Res. Found. Workshop* **2003**, *42*, 127–151.
(15) Kellenberger, E.; Rodrigo, J.; Muller, P.; Rognan, D. Comparative Evaluation of Eight Docking Tools for Docking and Virtual Screening Accuracy. *Proteins: Struct., Funct., Bioinf.* **2004**, *57*, 225–242.
(16) Willis, R. C. 2001: A Dock Odyssey. *Mod. Drug Discovery* **2001**, *4*, 26–28.
(17) Verdonk, M. L.; Berdini, V.; Harshorn, M. J.; Mooij, W. T. M.; Murray, C. W.; Taylor, R. D.; Watson, P. Virtual Screening Using Protein–Ligand Docking: Avoiding Artificial Enrichment. *J. Chem. Inf. Comput. Sci.* **2004**, *44*, 793–806.
(18) Charifson, P. S.; Corkery, J. J.; Murcko, M. A.; Walters, W. P. Consensus Scoring: A Method for Obtaining Improved Hit Rates from Docking Databases of Three-Dimensional Structures into Proteins. *J. Med. Chem.* **1999**, *42*, 5100–5109.
(19) Wang, R.; Wang, S. How Does Consensus Scoring Work for Virtual Library Screening? An Idealized Computer Experiment. *J. Chem. Inf. Comput. Sci.* **2001**, *41*, 1422–1426.

(20) Stahl, M.; Rarey, M. Detailed Analysis of Scoring Functions for Virtual Screening. *J. Med. Chem.* **2001**, *44*, 1035−1042.
(21) Clark, R. D.; Strizhev, A.; Leonard, J. M.; Blake, J. F.; Matthew, J. B. Consensus Scoring for Ligand/Protein Interactions. *J. Mol. Graphics Modell.* **2002**, *20*, 281−295.
(22) Wang, R.; Lu, Y.; Wang, S. Comparative Evaluation of 11 Scoring Functions for Molecular Docking. *J. Med. Chem.* **2003**, *46*, 2287−2303.
(23) Marsden, P. M.; Puvanendrampillai, D.; Mitchell, J. B. O.; Glen, R. C. Predicting Protein−Ligand Binding Affinities: A Low Scoring Game? *Org. Biomol. Chem.* **2004**, *2*, 3267−3273.
(24) Rarey, M.; Kramer, B.; Lengauer, T. Docking of Hydrophobic Ligand with Interaction-Based Matching Algorithms. *Bioinformatics* **1999**, *15*, 243−250.
(25) Kramer, B.; Rarey, M.; Lengauer, T. Evaluation of the FlexX Incremental Construction Algorithm for Protein−Ligand Docking. *Proteins: Struct., Funct., Genet.* **1999**, *37*, 228−241.
(26) Berman, H. M.; Westbrook, J.; Feng, Z.; Gilliland, G.; Bhat, T. N.; Weissig, H.; Shindyalov, I. N.; Bourne, P. E. The Protein Data Bank. *Nucleic Acids Res.* **2000**, *28*, 235−242.
(27) *SYBYL 6.9*; Tripos Inc.: St. Louis, MO, 2002.
(28) Halgren, T. A. Merck Molecular Force Field. I. Basis, Form, Scope, Parametrization, and Performance of MMFF94. *J. Comput. Chem.* **1996**, *17*, 490−519.
(29) *X-Score 1.1*; Department of Internal Medicine, University of Michigan Medical School: Ann Arbor, MI, 2003.
(30) Katsuki, M.; Chuang, V. T. G.; Nishi, K.; Kawahara, K.; Nakayama, H.; Yamaotsu, N.; Hirono, S.; Otagiri, M. Use of Photoaffinity Labeling and Site Directed Mutagenesis for Identification of Key Residue Responsible for Extraordinarily High Affinity Binding of UCN-01 in Human Alpha 1-Acid Glycoprotein. *J. Biol. Chem.* **2005**, *280*, 1384−1391.
(31) Bissantz, C.; Folkers, G.; Rognan, D. Protein-Based Virtual Screening of Chemical Databases. 1. Evaluation of Different Docking/Scoring Combinations. *J. Med. Chem.* **2000**, *43*, 4759−4767.
(32) Xiang, L.; Hodgkin, B.; Liu, Q.; Sedlock, D. Evaluation and Application of Multiple Scoring Functions for a Virtual Screening Experiment. *J. Comput.-Aided Mol. Des.* **2004**, *18*, 333−344.

CI050283K

# Discovery of Nonpeptidic Small-Molecule AP-1 Inhibitors: Lead Hopping Based on a Three-Dimensional Pharmacophore Model

Keiichi Tsuchida,*,† Hisaaki Chaki,‡ Tadakazu Takakura,† Hironori Kotsubo,‡ Tadashi Tanaka,† Yukihiko Aikawa,‡ Shunichi Shiozawa,#,⊥ and Shuichi Hirono§

*Discovery Laboratories and Research Laboratories, Toyama Chemical Co., Ltd., 4-1 Shimookui 2-chome, Toyama 930-8508, Japan, Department of Rheumatology, Faculty of Health Science, Kobe University School of Medicine, 7-10-2 Tomogaoka, Suma-ku, Kobe 654-0142, Japan, Rheumatic Disease Division, Kobe University Hospital, 7-5-2 Kusunoki-cho, Chuo-ku, Kobe 650-0017, Japan, and School of Pharmaceutical Sciences, Kitasato University, 5-9-1 Shirokane, Minato-ku, Tokyo 108-8641, Japan*

*Received June 13, 2005*

We designed and synthesized small-molecule activator protein-1 (AP-1) inhibitors based on a three-dimensional (3D) pharmacophore model that we had previously derived from a cyclic decapeptide exhibiting AP-1 inhibitory activity. New AP-1 inhibitors with a 1-thia-4-azaspiro[4.5]decane or a benzophenone scaffold, which inhibit the DNA-binding and transactivation activities of AP-1, were discovered using a "lead hopping" procedure. An additional investigation of the benzophenone analogues confirmed the reliability of the pharmacophore model, its utility to discover AP-1 inhibitors, and the potency of the benzophenone derivatives as a lead series.

## Introduction

Activator protein-1 (AP-1) is a transcription factor that has a crucial role in cellular signal transduction, as it is responsible for the induction of a number of genes that are involved in cell proliferation, differentiation, and immune and inflammatory responses.[1,2] It has been implicated in various diseases, such as rheumatoid arthritis.[3,4]

AP-1 contains members of the Fos and Jun families, which form either Jun-Jun homodimers or Fos-Jun heterodimers and bind to the consensus DNA sequence 5′-TGAGTCA-3′, which is known as the AP-1 binding site.[1] An investigation of the X-ray crystal structure of the basic region-leucine zipper (bZIP) domains of c-Fos and c-Jun bound to a DNA fragment containing the AP-1 binding site revealed that both domains form continuous α-helices, and the heterodimer grips the major groove of the DNA, similar to a pair of forceps.[5]

Natural products such as curcumin,[6] dihydroguaiaretic acid,[7] and an anthraquinone derivative[8] were reported to inhibit the binding of AP-1 to the AP-1 binding site. However, three-dimensional (3D) structural information about the AP-1 binding of these inhibitors that is necessary for structure-based drug design is not well-known. In a previous report,[9] we discovered a new cyclic disulfide decapeptide Ac-*cyclo*[Cys-Gly-Gln-Leu-Asp-Leu-Ala-Asp-Gly-Cys]-$NH_2$ (peptide **1**) that exhibits AP-1 inhibitory activity, using a de novo approach that exploited molecular modeling methods, such as molecular dynamics (MD) simulations, and docking studies based on the 3D structure of the bZIP domains derived from the X-ray structure.[5] Furthermore, we built a 3D pharmacophore model based on the chemical and structural features of peptide **1**. These data were obtained from an alanine scan and structural studies involving a combination of MD simulation of the bZIP−peptide **1** complex with explicit water molecules (Figure 1) and NMR measurements of the peptide in water.[9]

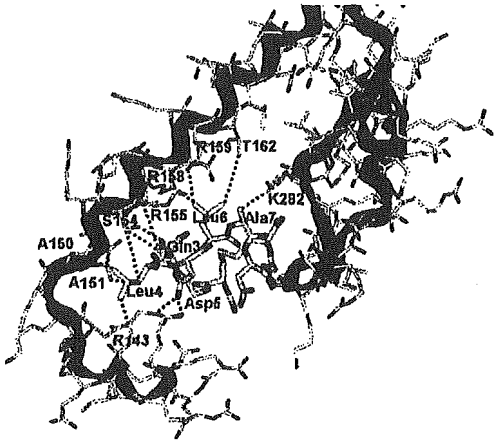


**Figure 1.** Binding model of peptide **1** (yellow) resulting from MD simulation. Ribbon representation of the basic domains (c-Fos, cyan; c-Jun, magenta). The residues of c-Fos and c-Jun that are involved in interactions are labeled with one-letter codes, and the residues of peptide **1** that are involved in interactions are labeled with three-letter codes. Red broken lines indicate putative hydrogen bonds and green broken lines indicate putative hydrophobic interactions. Hydrogen atoms are not shown for clarity.

Peptides generally have unfavorable properties for therapeutic drugs, such as poor bioavailability.[10] Several approaches have been reported to convert bioactive peptides into nonpeptidic drug candidates known as peptidomimetics.[10−12] In many cases, these peptidomimetics are peptide-like molecules, such as peptoids, and so further modifications are essential.

To avoid these problems, we designed nonpeptidic small molecules using a molecular modeling method based on a 3D pharmacophore model. This procedure could be described as "lead hopping" and has been employed as part of several recent in silico approaches.[13] There are two general computational approaches, de novo design and 3D database searching, to identify new lead candidates with desired biological activity using a pharmacophore model.[14] Although several successful

* To whom correspondence should be addressed. Phone: +81-76-431-8218. Fax: +81-76-431-8208. E-mail: keiichi_tuchida@toyama-chemical.co.jp.
† Discovery Laboratories, Toyama Chemical Co., Ltd.
‡ Research Laboratories, Toyama Chemical Co., Ltd.
# Kobe University School of Medicine.
⊥ Kobe University Hospital.
§ Kitasato University.

10.1021/jm050550d CCC: $33.50 
Published on Web 12/01/2005

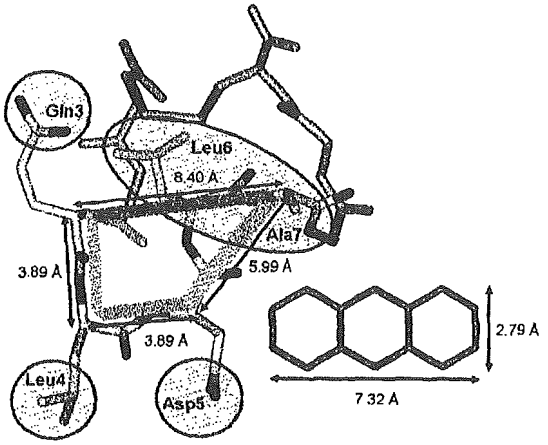


**Figure 2.** Pharmacophore model derived from peptide **1**. The pharmacophoric residues and the supplementary parts are colored yellow and gray, respectively. The pharmacophoric elements on peptide **1** are shown as circles and an ellipse in magenta. The main chain forms a trapezoid shape, the dimensions of which are shown by the arrows. An anthracene molecule of the same scale is depicted in green for a comparison of the sizes. Hydrogen atoms are not shown for clarity.

examples of these have been reported, the problems inherent in them have also been pointed out.[15,16] In de novo design, output structures are particularly apt to be difficult to synthesize.[15,16] In 3D database searching, novel structures cannot be obtained.[15] Thus, we chose to search the compound library in our company to identify synthetically accessible scaffolds before general 3D database searching. We succeeded in finding several good scaffolds in the library. These scaffolds are synthetically accessible and easy to modify by our organic chemists. Through design efforts based on these scaffolds, we discovered new AP-1 inhibitors: 1-thia-4-azaspiro[4.5]decane and benzophenone derivatives.

In the current paper, we describe the design by a lead-hopping strategy and synthesis of nonpeptidic AP-1 inhibitors and their inhibitory activities as evaluated by AP-1 binding and cell-based reporter gene assays.

**The Design of Nonpeptidic AP-1 Inhibitors. Lead-Hopping Strategy.** Our pharmacophore model of AP-1 binding compounds is illustrated in Figure 2, which shows the 3D arrangement of the side-chain functional groups of the Gln-Leu-Asp-Leu-Ala residues in peptide **1**.[9] A visual inspection revealed that the main chain of the five residues of peptide **1** has a $\beta$-turn-like conformation and a trapezoid shape (Figure 2). Its dimensions, which were measured as the distances between the $\alpha$-carbons of Gln3-Leu4, Leu4-Asp5, Asp5-Ala7, and Gln3-Ala7, are 3.89, 3.89, 5.99, and 8.40 Å, respectively. Thus, we decided to design candidate small molecules for synthesis and evaluation by combining a suitably sized scaffold placed onto the trapezoid structure with the corresponding pharmacophoric elements, which constitute pivotal functional groups within the side chains of the five pharmacophoric residues of peptide **1**, to retain the 3D arrangement in the pharmacophore model.

**Scaffold Design.** In general, it is assumed that a scaffold should have a certain level of rigidity to maintain the correct spatial arrangement of each of the pharmacophoric elements. In addition, the substitution position to which a pharmacophoric element might be connected via a suitable linker should be flexible to ensure synthetic feasibility. In a different perspective, at least three substituents for each pharmacophoric element could be introduced that would allow sufficient pharmacophoric interactions. As depicted in Figure 2, the trapezoid was as large as an anthracene molecule, which was therefore assumed to be the maximum size for a scaffold.

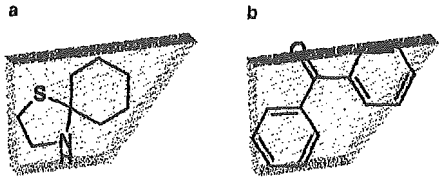


**Figure 3.** Fitting images of two scaffolds, 1-thia-4-azaspiro[4.5]decane (a) and benzophenone (b) to the trapezoid shown in Figure 2.

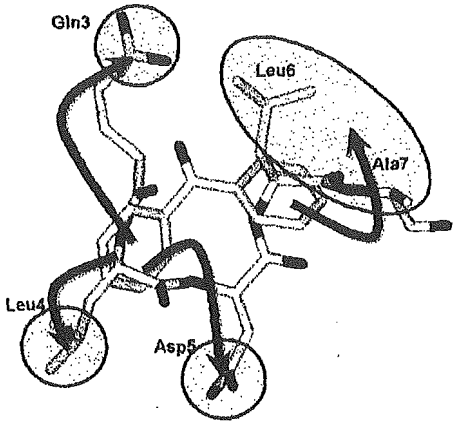


**Figure 4.** Illustration of the lead hopping of benzophenone. The superposition of the pharmacophoric residues of peptide **1** and the benzophenone scaffold is shown. The pharmacophoric elements on peptide **1** are shown as magenta-colored circles and an ellipse. The connections of the substituents from benzophenone are denoted by curved arrows.

Although the main chain of the five pharmacophoric residues of peptide **1** had a planar trapezoid shape, the pharmacophoric elements were not located on the same plane. Thus, to maintain the pharmacophoric arrangement, it was desirable that the scaffold was not planar, but rather was twisted and compact, within limits.

On the basis of these considerations, by searching our compound library, we selected the two scaffolds that are depicted in Figure 3: 1-thia-4-azaspiro[4.5]decane (a), and benzophenone (b) scaffolds.

**Definition of Pharmacophoric Elements.** Four pharmacophoric elements were defined from the five residues of the pharmacophore model: the carboxamide group of Gln3, the isobutyl group of Leu4, the carboxyl group of Asp5, and an isobutyl group that was adopted as a proxy for Leu6 and Ala7. The reason for using a proxy was that the two residues in question were adjacent to one another and could be regarded as one large hydrophobic element. Among these, the carboxyl group of Asp5 was regarded as a key pharmacophoric element, because substitution of the Asp5 had a significant effect in a previous alanine scan experiment;[9] we therefore assumed that an acidic group at this position was essential for interactions with the basic regions of the bZIP domains. In addition, this carboxyl group appeared to be the only charged group and might have conferred desirable features in terms of drug design. We therefore produced various combinations of three or four pharmacophoric elements, while ensuring that a carboxyl group was incorporated into the newly designed molecules.

**Scaffold Placement and Substitution Points.** Only those atoms on a scaffold for which the introduction of a suitable substituent was synthetically feasible were viewed as potential

Table 1. Chemical Structure of Compounds 2–5 and Their Inhibitory Activities against AP-1

| compd | structure | $IC_{50}$ (μM) binding assay[a] | $IC_{50}$ (μM) luciferase assay[b] |
|---|---|---|---|
| 1 | Ac-*c* [Cys-Gly-Gln-Leu-Asp-Leu-Ala-Asp-Gly-Cys]-$NH_2$ | 64 | NT[c] |
| 2 | 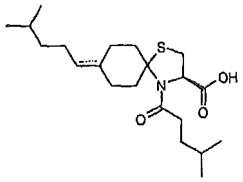 | 650 | 11.8 |
| 3 | 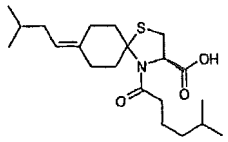 | 460 | 13.3 |
| 4 | 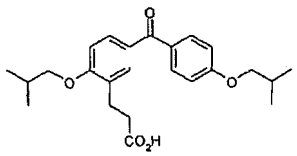 | 610 | 5.0 |
| 5 | 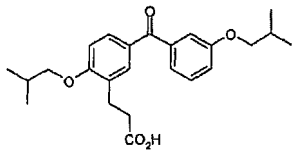 | 600 | 5.8 |

[a] Inhibition of the binding of the AP-1 bZIP peptide to synthetic oligonucleotides containing the AP-1 binding site. [b] Inhibition of the expression of AP-1-luciferase by TPA-stimulated NIH3T3 cells. [c] NT: not tested.

substitution points. Each scaffold was manually placed onto the trapezoid depicted in Figure 2 and interactively checked using a visual display. The position and orientation of the scaffolds were designed so that as many substitution points as possible were pointed in a favorable direction toward the corresponding pharmacophoric elements.

**Combination of Scaffold and Pharmacophore Elements.** The candidate molecules for the synthesis were constructed by connecting the relevant pharmacophoric elements to suitable substitution points on each scaffold via linkers.

An example of substituent introduction featuring benzophenone is shown in Figure 4. The connections between the pharmacophoric elements at suitable substitution points are indicated by curved arrows. In this case, the pharmacophoric elements corresponding to Gln3, Leu4, and Asp5 could be connected by any atoms on the left-hand ring of the scaffold via linkers. Likewise, the centroid of Leu6 and Ala7 could be connected from any atom on the right-hand ring. The lengths and types of linkers used were carefully selected, taking synthetic feasibility into consideration.

**Computational Evaluation of Designed Molecules.** We examined the various possible combinations of substitution points, and the lengths and types of linkers, so that each pharmacophoric element was well suited to the pharmacophore model. Each of the designed molecules was computationally evaluated to verify the fact that the 3D pharmacophore requirements were met by a low-energy conformer. Conformational analyses were carried out to obtain low-energy conformers. All unique conformers that were within 6 kcal $mol^{-1}$ of the lowest energy were collected for each of the designed molecules. The selected low-energy conformers were then systematically superimposed onto peptide **1** using the least-squares fit[17] of three or four of the pharmacophoric atoms: the δ-carbon atom of Gln3, the γ-carbon atoms of Leu4 and Asp5, and the centroid of the γ- and δ-carbon atoms of Leu6 and the β-carbon atom of Ala7. In addition, the overlapping volume between each conformer and the corresponding pharmacophoric residues in peptide **1**, and its ratio to the volume of the corresponding residues in peptide **1**, were calculated. Those compounds in which at least one conformer had a root-mean-square deviation

**Table 2.** Benzophenone Derivatives **4**, **6**–**13** and Their Inhibitory Activities in Binding Assay

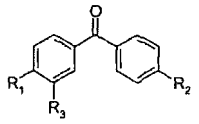

| compd | $R_1$ | $R_2$ | $R_3$ | % inhibition at 500 μM | % inhibition at 1 mM | $IC_{50}$ (μM)[a] |
|---|---|---|---|---|---|---|
| **4** | O$^t$Bu | O$^t$Bu | $CH_2CH_2CHO_2H$ | 28 | 91 | 610 |
| **6** | H | O$^t$Bu | $CH_2CH_2CHO_2H$ | 10 | 14 | >2000 |
| **7** | O$^t$Bu | H | $CH_2CH_2CHO_2H$ | 7 | 9 | >2000 |
| **8** | O$^t$Bu | O$^t$Bu | H | 3 | —[b] | ND[c] |
| **9** | O$^n$Pr | O$^t$Bu | $CH_2CH_2CHO_2H$ | 26 | 55 | 910 |
| **10** | O$^t$Bu | O$^n$Pr | $CH_2CH_2CHO_2H$ | 25 | 42 | 930 |
| **11** | $OCH_2Ph$ | O$^t$Bu | $CH_2CH_2CHO_2H$ | 51 | 97 | 420 |
| **12** | O$^t$Bu | $OCH_2Ph$ | $CH_2CH_2CHO_2H$ | 45 | —[b] | ND[c] |
| **13** | O$^t$Bu | O$^t$Bu | $CH_2CH_2CONH_2$ | 5 | —[b] | ND[c] |

[a] *50%* inhibition concentration was determined from the concentration–response curve (125–2000 μM). [b] % inhibition was not determined at this concentration due to precipitation. [c] ND: not determined.

**Scheme 1**[a]

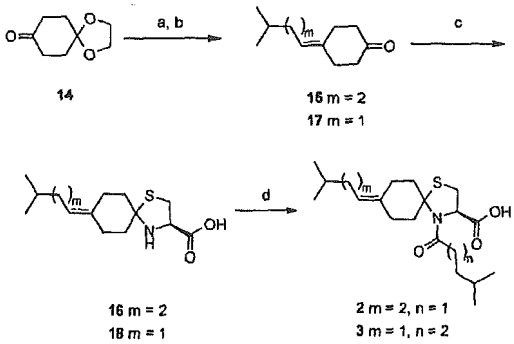


[a] Reagents: (a) $Me_2CHCH_2CH_2CH_2PPh_3Br$ (for **15**) or $Me_2CHCH_2CH_2$-$PPh_3I$ (for **17**), *n*-butyllithium, THF; (b) 6 M HCl, 1,4-dioxane; (c) L-cysteine, aq EtOH; (d) 4-methylpentanoic acid (for **2**) or 5-methylhexanoic acid (for **3**), oxalyl chloride, $Et_3N$, $CH_2Cl_2$.

(RMSD) value ≤ 1.0 Å under a three- or four-point superposition with the corresponding residues of peptide **1**, and an overlapping volume ratio ≥ 0.5, were selected as small-molecule inhibitor candidates for synthesis and biological evaluation.

**Biological Evaluation of the Compounds Synthesized.** The AP-1 inhibitory activities of the compounds synthesized were evaluated using enzyme-linked immunosorbent assay (ELISA)-based AP-1 DNA-binding and cell-based reporter assays (Table 1; compounds **2**–**5**).

Furthermore, the synthesis of benzophenone derivatives and the evaluation of their inhibitory activities were performed to verify our pharmacophore model (Table 2; compounds **6**–**13**).

## Chemistry

Synthesis of the (*R*)-4-(4-methylpentanoyl)-1-thia-4-azaspiro-[4.5]decane compound **2** was carried out as outlined in Scheme 1. The starting material, 1,4-cyclohexanedione monoethylene ketal (**14**), was subjected to the Wittig reaction with 4-methylpentyltriphenylphosphonium bromide and *n*-butyllithium to afford 4-(4-methylpentylidene)cyclohexanone (**15**) after an acid-catalyzed deprotection procedure. Treatment of **15** with L-cysteine in aqueous EtOH produced the spiro[cyclohexane-1,2′-thiazolidine] compound **16**, which was treated with 4-methylpentanoyl chloride in the presence of $Et_3N$ to provide the target molecule **2**.[18] The structurally analogous spiro compound **3**, 1-thia-4-azaspiro[4.5]decane-3-carboxylic acid, 8-(3-methylbutylidene)-4-(5-methylhexanoyl), was prepared by the same procedure.

**Scheme 2**[a]

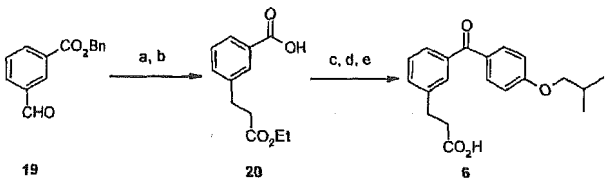


[a] Reagents: (a) $(EtO)_2P(O)CH_2CO_2Et$, NaH, DMF; (b) $H_2$, Pd–C, EtOH; (c) oxalyl chloride, DMF, $CH_2Cl_2$; (d) isobutoxybenzene, $AlCl_3$, $CH_2Cl_2$; (e) NaOH–$H_2O$, EtOH.

Syntheses of mono- and di-isobutoxy derivatives of 3-(3-benzoylphenyl)propionic acid (**4**–**7**) were carried out as illustrated in Schemes 2–4. 3-[3-(4-Isobutoxybenzoyl)phenyl]-propionic acid (**6**) was prepared via the Horner–Emmons reaction of benzyl 3-formylbenzoate (**19**) with ethyl diethylphosphonoacetate and NaH, which was followed by Pd–C-catalyzed hydrogenation to yield 3-(ethoxycarbonylethyl)benzoic acid (**20**). The corresponding acid chloride generated by treatment with oxalyl chloride was allowed to react with isobutoxybenzene[19] in the presence of $AlCl_3$ in $CH_2Cl_2$ to give an ethyl ester, which on alkaline ester hydrolysis provided compound **6** (Scheme 2). Compound **7** (Scheme 3), which is a regioisomer of the isobutoxy group of **6**, was prepared via isobutyl 3-(2-isobutyloxyphenyl)propionate (**22**), which was subjected to a regioselective Friedel–Crafts benzoylation. Compound **22** was also employed for the synthesis of 3-[2-isobutoxy-5-(4-isobutoxybenzoyl)phenyl]propionic acid (**4**). The regioselective formylation reaction[20] of **22** followed by Na$ClO_2$–$H_2O_2$ oxidation[21] afforded the monocarboxylic acid **23**, and coupling its acyl chloride with isobutoxybenzene afforded compound **4**. The regioisomer **5**, 3-[2-isobutoxy-5-(3-isobutoxybenzoyl)phenyl]propionic acid, was prepared via coupling of **22** with the acyl chloride of 3-isobutoxybenzoic acid (**25**) in the presence of $AlCl_3$ (Scheme 4).

Exchange of either one of the two isobutyloxy groups in **4** with a propyloxy or benzyloxy ether moiety was also considered as outlined in Scheme 5. The methyl ester of **4** (compound **26**) was subjected to $AlCl_3$-catalyzed lactonization accompanied by cleavage of the isobutoxy linkage to produce 6-(4-hydroxybenzoyl)-3,4-dihydrocoumarin (**27**). The liberated phenolic hydroxyl group was then subjected to the Mitsunobu reaction with $R^2$-OH (2-methylpropanol, propanol, or benzyl alcohol) in the presence of diisopropyl azodicarboxylate (DIAD) and triphenylphosphine in tetrahydrofuran (THF) followed by MeONa-

**Scheme 3**[a]

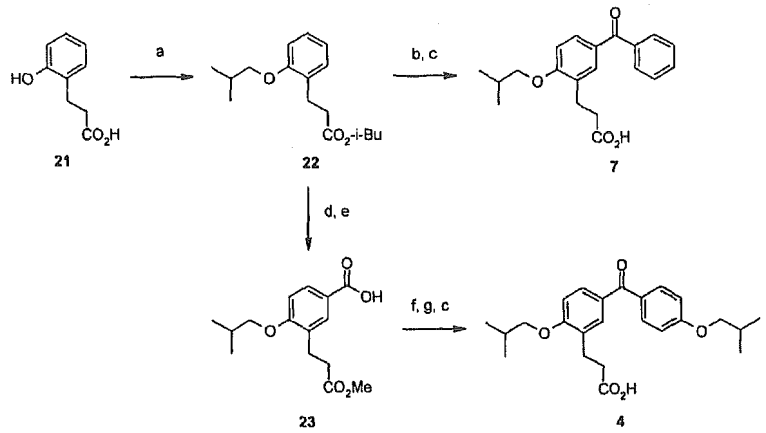


[a] Reagents: (a) isobutyl bromide, $K_2CO_3$, DMF; (b) benzoyl chloride, $AlCl_3$, $CH_2Cl_2$; (c) NaOH−$H_2O$, acetone (for **4**) or EtOH (for **7**); (d) $Cl_2CHOMe$, $AlCl_3$, $CH_2Cl_2$, then MeOH, Δ; (e) $NaClO_2$, $H_2O_2$, $NaH_2PO_4$, *aq.* MeCN; (f) oxalyl chloride, DMF, $CH_2Cl_2$; (g) isobutoxybenzene, $AlCl_3$, $CH_2Cl_2$.

**Scheme 4**[a]

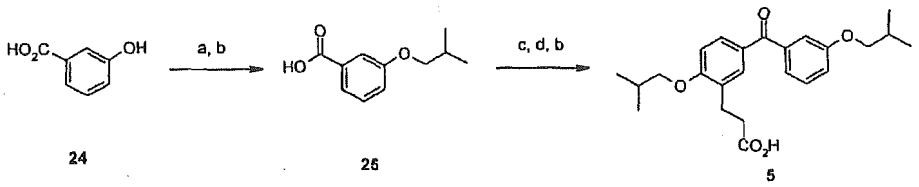


[a] Reagents: (a) isobutyl bromide, $K_2CO_3$, DMF; (b) NaOH−$H_2O$, acetone; (c) oxalyl chloride, DMF, $CH_2Cl_2$; (d) compound **22**, $AlCl_3$, $CH_2Cl_2$.

**Scheme 5**[a]

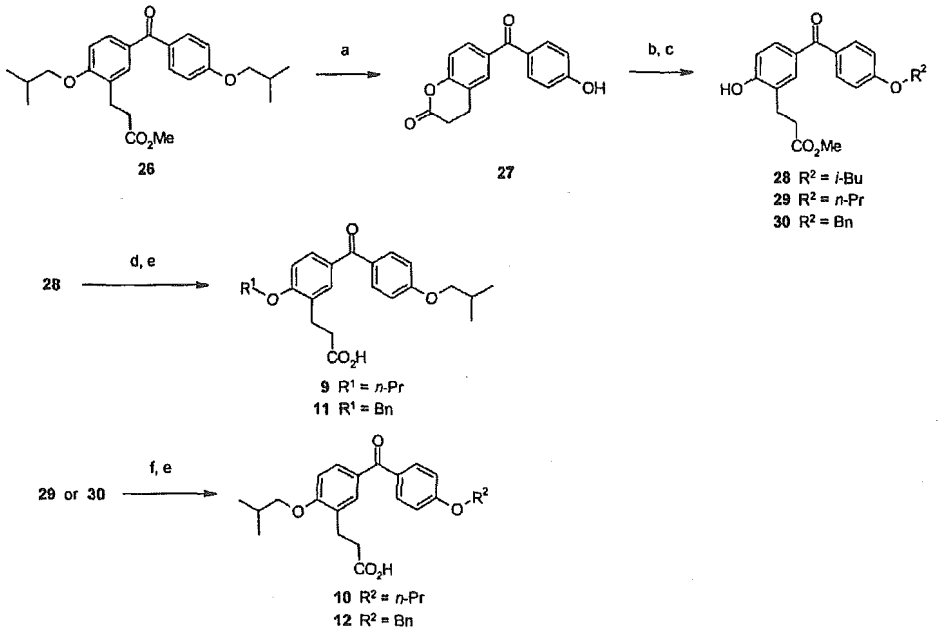


[a] Reagents: (a) $AlCl_3$, 1,2-dichloroethane; (b) $R^2$-OH, DIAD, $Ph_3P$, THF; (c) MeONa-MeOH, THF; (d) $R^1$-Br, $K_2CO_3$, DMF; (e) NaOH−$H_2O$, acetone; (f) isobutyl bromide, $K_2CO_3$, DMF.

catalyzed methanolysis to yield the corresponding alkyl ethers **28**−**30**. Compound **28** was alkylated with $R^1$-Br (propyl bromide or benzyl bromide), followed by hydrolysis with alkali to yield **9** and **11** as depicted in Scheme 5. The regioisomeric analogues **10** and **12** were prepared similarly via **29** ($R^2$ = propyl) and **30** ($R^2$ = benzyl), respectively.

Synthesis of carboxamide of **4** (compound **13**) was carried out as outlined in Scheme 6. Compound **4** was treated with oxalyl chloride and catalytic DMF leading to the acid chloride,

**Scheme 6**[a]

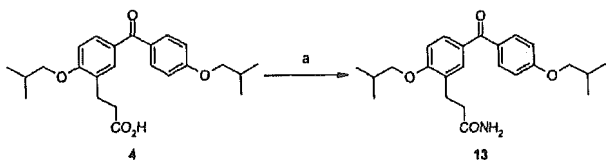


[a] Reagents: (a) oxalyl chloride, DMF, THF, then $NH_4OH$.

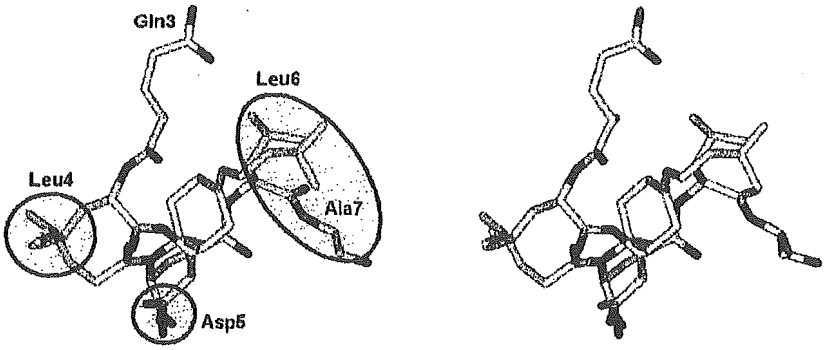


**Figure 5.** Stereoview of the superposition of Leu-Asp-Leu-Ala of peptide **1** (yellow) with compound **2** (white). The fitted points are shown as magenta-colored circles and an ellipse. Hydrogen atoms are not shown for clarity.

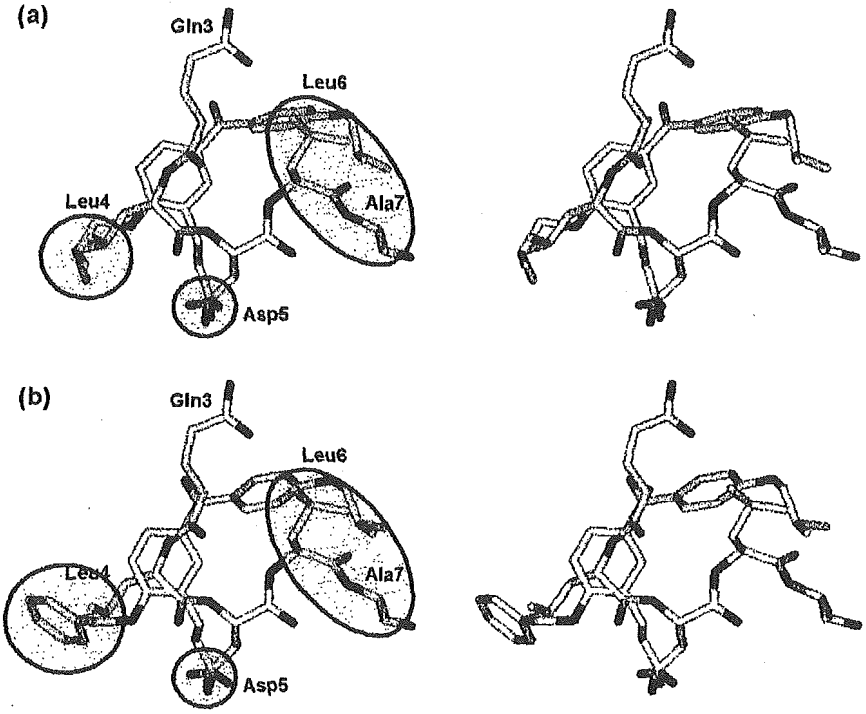


**Figure 6.** Stereoviews of the superposition of Leu-Asp-Leu-Ala of peptide **1** (yellow) with (a) compound **4** (white) and (b) compound **11** (white). The fitted points are shown as magenta-colored circles and an ellipse. Hydrogen atoms are not shown for clarity.

which was converted to propionamide **13** with ammonium hydroxide. Bis(4-isobutoxyphenyl)methanone (**8**) was prepared from commercially purchased bis(4-hydroxyphenyl)methanone by O-isobutylation with isobutyl bromide and $K_2CO_3$ in DMF.

## Results and Discussion

**Evaluation of Designed Compounds.** The designed compounds were synthesized and evaluated using an ELISA-based AP-1 DNA-binding assay. Among these, compounds **2** and **3** bearing 1-thia-4-azaspiro[4.5]decane as a scaffold, and compounds **4** and **5**, bearing benzophenone as a scaffold, inhibited the binding of AP-1 bZIP and oligonucleotides containing the AP-1 binding site (Table 1; $IC_{50}$ = 460−650 $\mu$M). The three pharmacophoric elements of these compounds corresponded to Leu4, Asp5, and the centroid of Leu6 and Ala7 of peptide **1**. As examples, the best-fit superpositions of compounds **2** and **4** onto peptide **1** based on the pharmacophore model are shown in Figures 5 and 6a, respectively. The three pairs of pharmacophoric points that were used for overlapping are shown as circles and an ellipse in these figures. The three overlapped points within compound **2** were the carbon atom of the carboxyl group plus the carbon atoms at the branched positions of the 4-methylpentanoyl and 4-methylpentylidene groups. The RMSD value resulting from the superposition of the three pharmacophoric points was 0.89 Å, and the energy of this best-fitted conformer relative to the lowest energy was 2.01 kcal $mol^{-1}$. The three overlapped points within compound **4** were the carbon atom of the carboxyl group plus the carbon atoms at the branched positions of the isobutyl groups. The RMSD value resulting from the superposition of the three pharmacophoric points was 0.92 Å, and the energy of this best-fitted conformer relative to the lowest energy was 2.46 kcal $mol^{-1}$. The structural isomers **2** and **3**, in which the lengths of methylene linkers between the 1-thia-4-azaspiro[4.5]decane scaffold and each isobutyl pharmacophore element were different, showed similar activity. The RMSD value obtained by the best-fit superposition of compound **3** and peptide **1** was 0.64 Å, and the energy of the best-fitted conformer relative to the lowest energy was 1.73 kcal $mol^{-1}$; thus the 3D pharmacophore requirement was met by compound **3**, as well as compound **2**. Because compounds

4 and 5, in which only the substitution position of an isobutoxy moiety corresponding to the centroid of Leu6 and Ala7 differed, showed similar activity, there might be some allowance in the hydrophobic region of the pharmacophore. This was consistent with our assumption that Leu6 and Ala7 comprised one large hydrophobic element. These small-molecule compounds showed lower inhibitory activity than peptide **1** ($IC_{50}$ = 64 $\mu$M). The results would be acceptable, given that these compounds have only three pharmacophore elements compared to the cyclic decapeptide.

Subsequently, we evaluated the effects of these compounds on the transactivation activity of AP-1 using a cell-based AP-1 reporter gene assay (Table 1). Compounds **2**−**5** showed dose-dependent inhibitory activities in this assay, similar to AP-1 DNA-binding inhibition. Thus, taking into account both the inhibitory activities and synthetic feasibility, we carried out further structural development of the benzophenone derivatives.

**Conversion of Substituents on Benzophenone Derivatives.** To verify the pharmacophoric elements, we designed and synthesized several derivatives based on compound **4**, and evaluated their inhibitory activities on AP-1 DNA-binding (Table 2).

The conversion of each substituent of compound **4** to hydrogen (compounds **6**−**8**) resulted in a considerable loss of inhibitory activity in the binding assay; thus, the importance of the three pharmacophore elements was confirmed.

In addition, the conversion of each isobutoxy group to an *n*-propoxy group (compounds **9** and **10**) resulted in a moderate loss of inhibitory activity at 1 mM. This finding may suggest a requirement for bulkiness of the branched chain alkyl groups.

Furthermore, compounds **11** and **12**, in which each isobutoxy group was substituted with a benzyloxy group, showed similar inhibitory activities to compound **4**, which implied that both aliphatic and aromatic substituents were acceptable hydrophobic elements at this position. The best-fit superposition of compound **11** and peptide **1** is shown in Figure 6b. The three overlapped points within compound **11** are the carbon atom of the carboxyl group, the carbon atom at the branched position of the isobutyl group, and the carbon atom at the root of the benzene ring in the benzyl group. The RMSD value obtained by the superposition of the three pharmacophoric points was 0.93 Å, and the energy of this best-fitted conformer relative to the lowest energy was 4.58 kcal mol$^{-1}$. The conformation and orientation of compound **11** were similar to those of compound **4** (Figure 6).

Finally, we converted the $R_3$ substituent to investigate the importance of the carboxyl group. The conversion into carboxamide (compound **13**) resulted in a considerable loss of inhibitory activity. This result clearly demonstrates the significance of the ionic interactions. This appears to support our initial hypothesis that the basic lysine and/or arginine in the basic region of bZIP domains might take part in the interactions with peptide **1**.

The above-mentioned results demonstrate that the optimal arrangement of at least three pharmacophoric elements is fundamental. In addition, we suggest that it might be possible to enhance the inhibitory activity by the further introduction of a fourth pharmacophoric element corresponding to Gln3 of peptide **1** that showed more potent inhibitory activity.

## Conclusions

We converted cyclic peptide **1** to small-molecule AP-1 inhibitors using a lead-hopping approach based on a 3D pharmacophore model that was derived from the peptide. New AP-1 inhibitors, 1-thia-4-azaspiro[4.5]decane and benzophenone derivatives, were discovered using this combination of computational methods and medicinal chemistry intuition. Our study demonstrated the reliability of the 3D pharmacophore model and its utility in the discovery of AP-1 inhibitors. Additionally, the possibility of further improvement of the benzophenone derivatives was suggested by the results of the conversion of the substituents. The benzophenone derivatives were considered to be an attractive lead series, because they exhibited AP-1 inhibitory activities not only in the binding assay but also in the cell-based assay. The continuous optimization of this series might produce drugs that can be used against AP-1 for the treatment of various diseases.

## Experimental Section

**Molecular Modeling.** All molecular modeling was performed using the SYBYL software package version 6.5[22] running on a Silicon Graphics Power Indigo2 workstation. All of the compounds designed for use in this study were built using the SKETCH module. The carboxyl group of the designed compounds was deprotonated to imitate physiological conditions. The designed compounds were minimized using the Powell method in the MAXIMIN2 module of SYBYL to reach a final convergence of 0.01 kcal mol$^{-1}$ Å$^{-1}$; the MMFF94 force field and the MMFF94 charges[23] were employed for the energy minimizations. Electrostatic interactions were taken into consideration using a distance-based dielectric constant of 78.3 to simulate an aqueous environment.

Conformational analysis of each of the designed compounds was carried out using the Random Search module implemented in SYBYL. An absolute energy cutoff of 300 kcal mol$^{-1}$ was used to remove high energy conformations. The energy values during the optimization were computed with the MMFF94 force field and the MMFF94 charges. The number of maximum cycles was set to 1000. Within each cycle, the bonds that were defined as rotatable were set to random torsion angles and the compounds were then minimized. The number of maximum hits was set to 6. Unique conformers were distinguished by setting a RMS threshold of 0.2 Å, with chirality checking if necessary. The systematical superposition of collected low-energy conformers was carried out using the FIT routine in SYBYL.

The overlapping volume and the volume of the corresponding residues in peptide **1** as a template were calculated using the MVOLUME and VOLUME routines in SYBYL, respectively.

**Chemistry.** Melting points were determined using a B-545 melting point apparatus (Büchi Lab., Flawil, Switzerland) and were uncorrected. Proton NMR ($^1$H NMR) spectra were recorded on a JEOL JNM-AL 400 spectrometer (JEOL Ltd., Tokyo, Japan) using tetramethylsilane as the internal standard. Chemical shifts are reported in ppm (δ units), and the signal patterns are designated as s (singlet), d (doublet), t (triplet), q (quartet), m (multiplet), and br (broad). Column chromatography was carried out using PSQ100B silica gel of 75−200 $\mu$m (Fuji Silysia Chemical, Aichi, Japan). Low-resolution mass spectra (MS) were obtained on a Hitachi M-8000 mass spectrometer system equipped with an electrospray ionization interface (Hitachi Ltd., Tokyo, Japan). Elemental analysis (C, H, and N) was performed at Toyama Industrial Technology Center (Toyama, Japan), and all results were within ±0.4% of the theoretical values. Unless otherwise noted, all solvents, chemicals, and reagents were obtained commercially and used without purification. Peptide **1** has been previously described.[9]

**4-(4-Methylpentylidene)cyclohexanone (15).** To a stirred and cooled (−45 °C) suspension of 4-methylpentyltriphenylphosphonium bromide (13.1 g, 30.7 mmol) in THF (40 mL) was added dropwise *n*-butyllithium (1.6 M in hexane, 19.2 mL, 30.7 mmol). The mixture was then warmed to 0 °C over 20 min. A solution of 1,4-cyclohexanedione monoethylene ketal (**14**) (4.00 g, 25.6 mmol) in THF (20 mL) was added dropwise to the resulting phosphorane solution at 0−5 °C. Subsequently, the reaction mixture was allowed to warm to room temperature and was stirred for 1 h. The mixture was quenched with water (100 mL) and extracted with EtOAc (1

× 100 mL). The aqueous layer was extracted with EtOAc (1 × 50 mL). The combined organic extracts were washed with water (1 × 100 mL) and brine (1 × 100 mL), dried over $MgSO_4$, and concentrated under reduced pressure. The residue was purified by chromatography (silica gel 150 g, 5:1 hexane/EtOAc) to give 8-(4-methylpentylidene)-1,4-dioxaspiro[4.5]decane (5.40 g, 94%) as a colorless oil: $^1$H NMR (400 MHz, $CDCl_3$) $\delta$ 0.87 (6H, d, $J$ = 6.6 Hz), 1.21 (2H, q, $J$ = 7.5 Hz), 1.46−1.62 (1H, m), 1.62−1.72 (4H, m), 1.99 (2H, q, $J$ = 7.5 Hz), 2.21 (2H, t, $J$ = 6.3 Hz), 2.27 (2H, t, $J$ = 6.5 Hz), 3.97 (4H, s), 5.13 (1H, t, $J$ = 7.5 Hz).

A mixture of the ketal (1.00 g, 4.46 mmol) obtained above and 6 M HCl (5 mL) in 1,4-dioxane (10 mL) was stirred at room temperature for 9 h before dilution with $CHCl_3$ (50 mL) and water (30 mL). The aqueous layer separated was extracted with $CHCl_3$ (1 × 30 mL), and the combined organic extracts were washed with water (1 × 30 mL) and brine (1 × 30 mL), dried over $MgSO_4$, and concentrated under reduced pressure. The residue was purified by chromatography (silica gel 100 g, 10:1 hexane/EtOAc) to give **15** (0.77 g, 96%) as a colorless oil: $^1$H NMR (400 MHz, $CDCl_3$) $\delta$ 0.90 (6H, d, $J$ = 6.6 Hz), 1.16−1.32 (2H, m), 1.48−1.66 (1H, m), 2.04 (2H, q, $J$ = 7.6 Hz), 2.36−2.56 (8H, m), 5.30−5.38 (1H, m).

**4-(3-Methylbutylidene)cyclohexanone (17).** Compound **14** was treated by the procedure described for **15** except using 3-methylbutyltriphenylphosphonium iodide to afford **17** (65%) as a colorless oil: $^1$H NMR (400 MHz, $CDCl_3$) $\delta$ 0.91 (6H, d, $J$ = 6.6 Hz), 1.56−1.72 (1H, m), 1.90−1.97 (2H, m), 2.36−2.54 (8H, m), 5.37 (1H, t, $J$ = 7.3 Hz); MS $m/z$ 167 $(M + H)^+$.

**(*R*)-8-(4-Methylpentylidene)-1-thia-4-azaspiro[4.5]decane-3-carboxylic Acid (16).** A mixture of **15** (1.20 g, 6.66 mmol) and L-cysteine (1.21 g, 9.99 mmol) in a mixture of 7:3 EtOH/water (36 mL) was stirred at room temperature for 3 h and at 40 °C for 5 h. The reaction mixture was evaporated under reduced pressure before dilution with water (100 mL). The product precipitated was collected by filtration and washed with water (3 × 30 mL) and hexane (3 × 30 mL) to afford **16** (1.18 g, 63%) as a light brown solid: $^1$H NMR (400 MHz, $CDCl_3$) $\delta$ 0.88 (6H, d, $J$ = 6.6 Hz), 1.20 (2H, q, $J$ = 7.3 Hz), 1.46−1.60 (1H, m), 1.84−2.64 (10H, m), 3.22−3.34 (1H, m), 3.36−3.50 (1H, m), 4.33 (1H, t, $J$ = 7.2 Hz), 5.10−5.22 (1H, m), 5.30−5.70 (2H, br); MS $m/z$ 284 $(M + H)^+$, 282 $(M - H)^-$.

**(*R*)-8-(3-Methylbutylidene)-1-thia-4-azaspiro[4.5]decane-3-carboxylic Acid (18).** Compound **17** (5.00 g, 30.1 mmol) was treated by the procedure described for **16** to afford **18** (4.40 g, 54%) as a white solid: $^1$H NMR (400 MHz, $CDCl_3$) $\delta$ 0.87 (6H, d, $J$ = 6.3 Hz), 1.50−1.64 (1H, m), 1.82−2.14 (6H, m), 2.16−2.64 (4H, m), 3.22−3.32 (1H, m), 3.42 (1H, dd, $J$ = 11.3, 7.4 Hz), 3.78 (2H, br s), 4.32 (1H, t, $J$ = 7.4 Hz), 5.19 (1H, t, $J$ = 7.3 Hz); MS $m/z$ 268 $(M - H)^-$.

**(*R*)-4-(4-Methylpentanoyl)-8-(4-methylpentylidene)-1-thia-4-azaspiro[4.5]decane-3-carboxylic Acid (2).** To a stirred solution of 4-methylpentanoic acid (225 mg, 1.94 mmol) in $CH_2Cl_2$ (5 mL) at room temperature was added dropwise oxalyl chloride (246 mg, 1.94 mmol) followed by the addition of DMF (50 $\mu$L), and the mixture was stirred at the same temperature for 2 h. The mixture was cooled in an ice bath before the sequential addition of **16** (500 mg, 1.76 mmol) and $Et_3N$ (535 mg, 5.29 mmol), and then the mixture was stirred at room temperature for 2 h. The resulting mixture was treated with $CHCl_3$ (30 mL) and water (30 mL), followed by acidification to pH 2 with 6 M HCl, and the layers were separated. The aqueous layer was extracted with $CHCl_3$ (30 mL), and the combined organic extracts were washed with water (1 × 30 mL) and brine (1 × 30 mL), dried over $MgSO_4$, and concentrated under reduced pressure. The residue was purified by chromatography (silica gel 50 g, 10:1 $CHCl_3$/MeOH) to give **2** (380 mg, 56%) as a white solid, which was crystallized from $CH_2Cl_2$/hexane to give colorless crystals, mp 144−145 °C: $^1$H NMR (400 MHz, $CDCl_3$) $\delta$ 0.87 (6H, d, $J$ = 6.6 Hz), 0.88 (6H, d, $J$ = 5.6 Hz), 1.20 (2H, q, $J$ = 7.0 Hz), 1.34−1.78 (5H, m), 1.86−2.72 (9H, m), 2.84−3.38 (4H, m), 4.90−5.02 (1H, m), 5.06−5.16 (1H, m), 5.25−5.45 (1H, br); MS $m/z$ 381 $(M - H)^-$. Anal. ($C_{21}H_{35}NO_3S$) C, H, N.

**(*R*)-8-(3-Methylbutylidene)-4-(5-methylhexanoyl)-1-thia-4-azaspiro[4.5]decane-3-carboxylic Acid (3).** Compound **18** (500 mg, 1.86 mmol) was treated by the procedure described for **2** except using 5-methylhexanoic acid to afford **3** (305 mg, 43%) as a white solid, which was crystallized from $CH_2Cl_2$/hexane to give colorless crystals, mp 135−138 °C: $^1$H NMR (400 MHz, $CDCl_3$) $\delta$ 0.87 (12H, d, $J$ = 6.8 Hz), 1.10−1.24 (2H, m), 1.48−1.74 (5H, m), 1.76−2.50 (7H, m), 2.56−2.72 (1H, m), 2.84−3.34 (5H, m), 4.90−5.00 (1H, m), 5.10−5.20 (1H, m); MS $m/z$ 382 $(M + H)^+$, 380 $(M - H)^-$. Anal. ($C_{21}H_{35}NO_3S$) C, H, N.

**3-(2-Ethoxycarbonylethyl)benzoic Acid (20).** To a stirred suspension of NaH (60% dispersion in mineral oil, 1.37 g, 34.3 mmol) in DMF (75 mL) at 10−15 °C was added dropwise ethyl diethylphosphonoacetate (7.69 g, 34.3 mmol). The mixture was then stirred at room temperature for 30 min. To the stirred and ice-cooled mixture was added dropwise benzyl 3-formylbenzoate (**19**) (7.50 g, 31.2 mmol) before being stirred at room temperature for 30 min. The reaction mixture was poured into a mixture of EtOAc (100 mL) and 1 M HCl (50 mL), and the aqueous layer separated was extracted with EtOAc (1 × 50 mL). The organic extracts were washed with water (1 × 100 mL) and brine (1 × 100 mL), dried over $MgSO_4$, and concentrated under reduced pressure. The residue was purified by chromatography (silica gel 100 g, 3:1 hexane/EtOAc) to give benzyl 3-((*E*)-2-ethoxycarbonylvinyl)benzoate (9.12 g, 94%) as a colorless oil: $^1$H NMR (400 MHz, $CDCl_3$) $\delta$ 1.34 (3H, t, $J$ = 7.1 Hz), 4.27 (2H, q, $J$ = 7.1 Hz), 5.38 (2H, s), 6.50 (1H, d, $J$ = 16.0 Hz), 7.31−7.56 (6H, m), 7.70 (1H, d, $J$ = 8.1 Hz), 7.70 (1H, d, $J$ = 16.0 Hz), 8.08 (1H, d, $J$ = 7.8 Hz), 8.22 (1H, s); MS $m/z$ 311 $(M + H)^+$.

A suspension of the $\alpha,\beta$-unsaturated ester (8.50 g, 274 mmol) obtained above in EtOH (85 mL) was stirred at 40 °C under the atmospheric pressure of $H_2$ in the presence of 10% Pd−C (1.70 g). The mixture was filtered through Celite after 3 h, and the residue was washed with EtOH (3 × 20 mL). The filtrate was concentrated under reduced pressure to afford the semisolid residue, which was triturated with hexane (100 mL) to give **20** (5.87 g, 96%) as an off-white solid: $^1$H NMR (400 MHz, $CDCl_3$) $\delta$ 1.24 (3H, t, $J$ = 7.2 Hz), 2.67 (2H, t, $J$ = 7.7 Hz), 3.03 (2H, t, $J$ = 7.7 Hz), 4.14 (2H, q, $J$ = 7.2 Hz), 7.41 (1H, t, $J$ = 7.7 Hz), 7.47 (1H, d, $J$ = 7.7 Hz), 7.92−8.03 (2H, m); MS $m/z$ 221 $(M - H)^-$.

**Isobutyl 3-(2-Isobutoxyphenyl)propionate (22).** A mixture of 3-(2-hydroxyphenyl)propionic acid (**21**) (10.0 g, 60.2 mmol), $K_2CO_3$ (41.6 g, 301 mmol), and isobutyl bromide (33.0 g, 241 mmol) in DMF (100 mL) was heated with vigorous stirring at 140 °C for 1 h. After cooling to room temperature, the reaction mixture was treated with EtOAc (150 mL) and water (300 mL) followed by acidification to pH 4 with 6 M HCl. The organic extract was washed with water (1 × 50 mL) and brine (1 × 50 mL), dried over $MgSO_4$, and concentrated under reduced pressure. The residue was purified by chromatography (silica gel 300 g, 5:1 hexane/EtOAc) to give **22** (15.4 g, 92%) as a colorless oil: $^1$H NMR (400 MHz, $CDCl_3$) $\delta$ 0.91 (6H, d, $J$ = 7.1 Hz), 1.05 (6H, d, $J$ = 7.1 Hz), 1.84−1.96 (1H, m), 2.06−2.18 (1H, m), 2.63 (2H, t, $J$ = 7.9 Hz), 2.97 (2H, t, $J$ = 7.9 Hz), 3.74 (2H, d, $J$ = 6.4 Hz), 3.85 (2H, d, $J$ = 6.6 Hz), 6.78−6.88 (2H, m), 7.12−7.20 (2H, m); MS $m/z$ 279 $(M + H)^+$.

**4-Isobutoxy-3-(2-methoxycarbonylethyl)benzoic Acid (23).** To a stirred solution of **22** (10.0 g, 35.9 mmol) in $CH_2Cl_2$ (50 mL) at −30 °C were successively added $AlCl_3$ (9.58 g, 71.8 mmol) and dichloromethyl methyl ether (4.96 g, 43.1 mmol), and the mixture was stirred at −10 °C for 1 h. After addition of MeOH (50 mL), the resulting mixture was stirred under reflux for 2 h before cooling to room temperature. The reaction mixture was poured into ice−water (200 mL), and the organic layer was sequentially washed with 1 M HCl (1 × 50 mL) and water (1 × 50 mL), and concentrated under reduced pressure to give aldehyde as a brown oil, which was used without further purification. The aldehyde thus obtained was dissolved in $CH_3CN$ (20 mL). To the stirred solution were added a solution of $NaH_2PO_4 \cdot 2H_2O$ (15.1 g, 96.8 mmol) in water (20 mL) and 30% aqueous $H_2O_2$ (6.11 g, 53.9 mmol) in sequence. A solution of $NaClO_2$ (80% purity, 6.50 g, 57.5 mmol) in water (10 mL) was added dropwise over 10 min to the ice-cooled

mixture with stirring before being stirred at room temperature for 1 h. The solid material that had precipitated during the reaction was filtered and washed with water (2 × 20 mL) to give **23** (7.32 g, 73%) as a pale yellow solid: $^1$H NMR (400 MHz, $CDCl_3$) $\delta$ 1.06 (6H, d, $J$ = 6.6 Hz), 2.08−2.22 (1H, m), 2.64 (2H, t, $J$ = 7.8 Hz), 3.00 (2H, t, $J$ = 7.8 Hz), 3.69 (3H, s), 3.82 (2H, d, $J$ = 6.6 Hz), 6.86 (1H, d, $J$ = 8.7 Hz), 7.91 (1H, d, $J$ = 2.2 Hz), 7.98 (1H, dd, $J$ = 8.7, 2.2 Hz); MS $m/z$ 279 $(M - H)^-$.

**3-Isobutoxybenzoic Acid (25).** A mixture of 3-hydroxybenzoic acid (**24**) (10.0 g, 72.4 mmol), $K_2CO_3$ (25.0 g, 181 mmol), and isobutyl bromide (29.8 g, 217 mmol) in DMF (100 mL) was heated with stirring at 120 °C for 2 h. The reaction mixture was then cooled to room temperature, treated with water (300 mL) followed by acidification to pH 4 with 6 M HCl, and extracted with EtOAc (100 mL). The organic layer was washed with water (1 × 100 mL) and brine (1 × 100 mL), dried over $MgSO_4$, and evaporated under reduced pressure to afford di-O-isobutylated product as a pale yellow oil. The di-O-isobutylated product thus obtained was dissolved in acetone (100 mL), and then 20 wt % aqueous NaOH (50.0 g) was added to the mixture at room temperature. The reaction mixture was allowed to cool to room temperature after being stirred at 50 °C for 2 h, and then water (300 mL) was added. The mixture was acidified to pH 1 with 12 M HCl and stirred at room temperature for 30 min, and the resulting precipitate was collected by filtration and washed with water (2 × 50 mL) to give **25** (9.85 g, 70%) as a white solid: $^1$H NMR (400 MHz, $CDCl_3$) $\delta$ 1.05 (6H, d, $J$ = 6.4 Hz), 2.04−2.18 (1H, m), 3.78 (2H, d, $J$ = 6.6 Hz), 7.16 (1H, ddd, $J$ = 7.9, 2.6, 0.5 Hz), 7.37 (1H, t, $J$ = 7.9 Hz), 7.62 (1H, dd, $J$ = 2.6, 1.6 Hz), 7.70 (1H, d, $J$ = 7.9 Hz); MS $m/z$ 193 $(M - H)^-$.

**3-[2-Isobutoxy-5-(4-isobutoxybenzoyl)phenyl]propionic Acid (4).** To a stirred solution of **23** (2.00 g, 7.13 mmol) and DMF (0.1 mL) in $CH_2Cl_2$ (20 mL) at room temperature was added oxalyl chloride (1.09 g, 8.59 mmol). After continuous stirring for 1 h, the mixture was cooled with ice−water before the sequential addition of $AlCl_3$ (2.09 g, 15.7 mmol) and isobutoxybenzene (1.29 g, 8.59 mmol). After being stirred at 5−10 °C for 30 min, the reaction mixture was poured into a mixture of ice (20 g) and 6 M HCl (30 mL). The layers were separated, and the organic layer was washed with water (1 × 20 mL) and brine (1 × 20 mL), dried over $MgSO_4$, and concentrated under reduced pressure. The residue was purified by chromatography (silica gel 50 g, 5:1 hexane/EtOAc) to give methyl 3-[2-isobutoxy-5-(4-isobutoxybenzoyl)phenyl]propionate (**26**) (2.36 g, 80%) as a white crystalline solid, mp 78−79 °C: $^1$H NMR (400 MHz, $CDCl_3$) $\delta$ 1.05 (6H, d, $J$ = 6.8 Hz), 1.07 (6H, d, $J$ = 6.8 Hz), 2.06−2.22 (2H, m), 2.64 (2H, t, $J$ = 7.8 Hz), 3.00 (2H, t, $J$ = 7.8 Hz), 3.67 (3H, s), 3.80 (2H, d, $J$ = 6.6 Hz), 3.82 (2H, d, $J$ = 6.3 Hz), 6.87 (1H, d, $J$ = 8.3 Hz), 6.95 (2H, d, $J$ = 8.7 Hz), 7.64 (1H, d, $J$ = 2.0 Hz), 7.67 (1H, dd, $J$ = 8.3, 2.0 Hz), 7.76 (2H, d, $J$ = 8.7 Hz); MS $m/z$ 413 $(M + H)^+$.

A mixture of **26** (10.4 g, 25.2 mmol) and 20 wt % aqueous NaOH (10.4 g) in acetone (30 mL) was stirred at 50 °C for 2 h before dilution with water (100 mL). The product that was precipitated by acidification to pH 1 with 12 M HCl was collected by filtration and washed with water (2 × 50 mL) to afford **4** (9.44 g, 94%) as a white solid, which was crystallized from $CH_2Cl_2$/hexane to give colorless crystals, mp 102−103 °C: $^1$H NMR (400 MHz, $CDCl_3$) $\delta$ 1.04 (6H, d, $J$ = 6.6 Hz), 1.07 (6H, d, $J$ = 6.8 Hz), 2.06−2.22 (2H, m), 2.71 (2H, t, $J$ = 7.7 Hz), 3.00 (2H, t, $J$ = 7.7 Hz), 3.80 (2H, d, $J$ = 6.4 Hz), 3.82 (2H, d, $J$ = 6.6 Hz), 6.87 (1H, d, $J$ = 8.5 Hz), 6.95 (2H, d, $J$ = 8.8 Hz), 7.66 (1H, d, $J$ = 2.2 Hz), 7.69 (1H, dd, $J$ = 8.5, 2.2 Hz), 7.76 (2H, d, $J$ = 8.8 Hz); MS $m/z$ 397 $(M - H)^-$. Anal. ($C_{24}H_{30}O_5$) C, H.

**3-[2-Isobutoxy-5-(3-isobutoxybenzoyl)phenyl]propionic Acid (5).** Compounds **22** and **25** were treated by the procedure described for **4** to afford **5** (85%) as a white solid, which was crystallized from $CH_2Cl_2$/hexane to give colorless crystals, mp 77−78 °C: $^1$H NMR (400 MHz, $CDCl_3$) $\delta$ 1.03 (6H, d, $J$ = 6.8 Hz), 1.07 (6H, d, $J$ = 6.8 Hz), 2.04−2.22 (2H, m), 2.70 (2H, t, $J$ = 7.7 Hz), 3.00 (2H, t, $J$ = 7.7 Hz), 3.77 (2H, d, $J$ = 6.4 Hz), 3.83 (2H, d, $J$ = 6.3 Hz), 6.87 (1H, d, $J$ = 9.3 Hz), 7.10 (1H, dd, $J$ = 7.9, 2.6 Hz), 7.22−7.32 (2H, m), 7.35 (1H, t, $J$ = 7.9 Hz), 7.68−7.78 (2H, m); MS $m/z$ 397 $(M - H)^-$. Anal. ($C_{24}H_{30}O_5$) C, H.

**3-[3-(4-Isobutoxybenzoyl)phenyl]propionic Acid (6).** Compound **20** and isobutoxybenzene were treated by the procedure described for **4** to afford **6** (77%) as a white solid, which was crystallized from $CH_2Cl_2$/hexane to give colorless crystals, mp 98−99 °C: $^1$H NMR (400 MHz, $CDCl_3$) $\delta$ 1.05 (6H, d, $J$ = 6.6 Hz), 2.06−2.18 (1H, m), 2.73 (2H, t, $J$ = 7.7 Hz), 3.03 (2H, t, $J$ = 7.7 Hz), 3.80 (2H, d, $J$ = 6.6 Hz), 6.95 (2H, d, $J$ = 8.8 Hz), 6.91−6.98 (3H, m), 7.36−7.46 (2H, m), 7.54−7.64 (2H, m), 7.80 (2H, d, $J$ = 8.8 Hz); MS $m/z$ 327 $(M + H)^+$, 325 $(M - H)^-$. Anal. ($C_{20}H_{22}O_4$) C, H.

**3-(5-Benzoyl-2-isobutoxyphenyl)propionic Acid (7).** Compound **22** and benzoyl chloride were treated by the procedure described for **4** to afford **7** (40%) as a white solid, which was crystallized from $CH_2Cl_2$/hexane to give colorless crystals, mp 95−97 °C: $^1$H NMR (400 MHz, $CDCl_3$) $\delta$ 1.07 (6H, d, $J$ = 6.6 Hz), 2.08−2.24 (1H, m), 2.71 (2H, t, $J$ = 7.7 Hz), 3.00 (2H, t, $J$ = 7.7 Hz), 3.83 (2H, d, $J$ = 6.3 Hz), 6.88 (1H, d, $J$ = 8.3 Hz), 7.44−7.52 (2H, m), 7.52−7.60 (1H, m), 7.68−7.80 (4H, m); MS $m/z$ 327 $(M + H)^+$, 325 $(M - H)^-$. Anal. ($C_{20}H_{22}O_4$) C, H.

**Methyl 3-[2-Hydroxy-5-(4-isobutoxybenzoyl)phenyl]propionate (28).** A mixture of **26** (1.00 g, 2.42 mmol) and $AlCl_3$ (1.94 g, 14.5 mmol) in 1,2-dichloroethane (10 mL) was stirred under reflux for 8 h before cooling to room temperature. The mixture was diluted with 2-butanone (50 mL) and then poured into a mixture of ice (15 g) and 12 M HCl (15 mL). The organic layer separated was sequentially washed with 1 M HCl (2 × 10 mL), water (1 × 10 mL), and brine (1 × 10 mL), dried over $MgSO_4$, and concentrated under reduced pressure. The residual solid was triturated with hexane (10 mL) to give **27** (0.55 g) as a pale red solid: $^1$H NMR (400 MHz, DMSO-$d_6$) $\delta$ 2.85 (2H, t, $J$ = 7.3 Hz), 3.08 (2H, t, $J$ = 7.3 Hz), 6.90 (2H, d, $J$ = 8.7 Hz), 7.19 (1H, d, $J$ = 8.3 Hz), 7.59 (1H, dd, $J$ = 8.3, 2.2 Hz), 7.65−7.67 (1H, m), 7.66 (2H, d, $J$ = 8.7 Hz), 10.43 (1H, s); MS $m/z$ 269 $(M + H)^-$, 267 $(M - H)^-$. To a suspension of **27** (0.55 g), isobutyl alcohol (0.18 g, 2.43 mmol), and triphenylphosphine (0.65 g, 2.48 mmol) in THF (6 mL) at temperatures below 40 °C was added dropwise DIAD (0.50 g, 2.47 mmol). After being stirred for 30 min, NaOMe (28 wt % in MeOH, 1.98 g, 10.3 mmol) was added dropwise to the ice-cooled mixture with stirring, and then the resulting mixture was stirred at room temperature for 30 min. The reaction mixture was treated with toluene (10 mL) and 1 M HCl (20 mL). The organic layer was sequentially washed with water (1 × 10 mL) and brine (1 × 10 mL), dried over $MgSO_4$, and concentrated under reduced pressure. The residue was purified by chromatography (silica gel 100 g, 4:1 hexane/EtOAc) to give **28** (0.60 g, 69%) as a white solid: $^1$H NMR (400 MHz, $CDCl_3$) $\delta$ 1.05 (6H, d, $J$ = 6.8 Hz), 2.06−2.18 (1H, m), 2.76 (2H, t, $J$ = 6.3 Hz), 2.95 (2H, t, $J$ = 6.3 Hz), 3.72 (3H, s), 3.80 (2H, d, $J$ = 6.6 Hz), 6.94 (1H, d, $J$ = 8.3 Hz), 6.95 (2H, d, $J$ = 8.7 Hz), 7.58 (1H, dd, $J$ = 8.3, 2.2 Hz), 7.63 (1H, d, $J$ = 2.2 Hz), 7.76 (2H, d, $J$ = 8.7 Hz), 7.95 (1H, br s); MS $m/z$ 357 $(M + H)^+$, 355 $(M - H)^-$.

**Methyl 3-[2-Hydroxy-5-(4-propoxybenzoyl)phenyl]propionate (29).** Compound **26** (1.00 g, 2.42 mmol) was treated by the procedure described for **28** except using $n$-propyl alcohol to afford **29** (0.56 g, 67%) as a white solid: $^1$H NMR (400 MHz, $CDCl_3$) $\delta$ 1.06 (3H, t, $J$ = 7.3 Hz), 1.80−1.90 (2H, m), 2.76 (2H, t, $J$ = 6.2 Hz), 2.95 (2H, t, $J$ = 6.2 Hz), 3.72 (3H, s), 4.00 (2H, t, $J$ = 6.6 Hz), 6.94 (1H, d, $J$ = 8.4 Hz), 6.95 (2H, d, $J$ = 8.8 Hz), 7.57 (1H, dd, $J$ = 8.4, 2.1 Hz), 7.63 (1H, d, $J$ = 2.1 Hz), 7.76 (2H, d, $J$ = 8.8 Hz), 7.92 (1H, s); MS $m/z$ 341 $(M - H)^-$.

**Methyl 3-[5-(4-Benzyloxybenzoyl)-2-hydroxyphenyl]propionate (30).** Compound **26** (1.00 g, 2.42 mmol) was treated by the procedure described for **28** except using benzyl alcohol to afford **30** (0.66 g, 70%) as a white solid: $^1$H NMR (400 MHz, $CDCl_3$) $\delta$ 2.76 (2H, t, $J$ = 6.2 Hz), 2.95 (2H, t, $J$ = 6.2 Hz), 3.72 (3H, s), 5.15 (2H, s), 6.94 (1H, d, $J$ = 8.4 Hz), 7.03 (2H, d, $J$ = 8.9 Hz), 7.32−7.48 (5H, m), 7.58 (1H, dd, $J$ = 8.4, 2.2 Hz), 7.64 (1H, d, $J$ = 2.2 Hz), 7.77 (2H, d, $J$ = 8.9 Hz), 7.94 (1H, s); MS $m/z$ 391 $(M + H)^+$, 389 $(M - H)^-$.

**3-[5-(4-Isobutoxybenzoyl)-2-propoxyphenyl]propionic Acid (9).** To a stirred suspension of **28** (3.00 g, 8.42 mmol) and $K_2CO_3$ (1.16 g, 8.39 mmol) in DMF (15 mL) at room temperature was added *n*-propyl bromide (1.55 g, 12.6 mmol), and the mixture was stirred at 90−100 °C for 1 h. After cooling to room temperature, the reaction mixture was treated with toluene (15 mL) and water (60 mL) followed by acidification to pH 4 with 6 M HCl. The organic layer was washed with water (1 × 20 mL) and brine (1 × 20 mL), dried over $MgSO_4$, and concentrated under reduced pressure. The residue was purified by chromatography (silica gel 75 g, 2:1 hexane/EtOAc) to give methyl 3-[5-(4-isobutoxybenzoyl)-2-propoxyphenyl]propionate (2.73 g, 81%) as a white solid: $^1$H NMR (400 MHz, $CDCl_3$) $\delta$ 1.02−1.12 (9H, m), 1.81−1.93 (2H, m), 2.00−2.20 (1H, m), 2.64 (2H, t, $J$ = 7.8 Hz), 2.99 (2H, t, $J$ = 7.8 Hz), 3.67 (3H, s), 3.80 (2H, d, $J$ = 6.3 Hz), 4.02 (2H, t, $J$ = 6.3 Hz), 6.87 (1H, d, $J$ = 8.4 Hz), 6.95 (2H, d, $J$ = 8.7 Hz), 7.64 (1H, d, $J$ = 2.2 Hz), 7.67 (1H, dd, $J$ = 8.4, 2.2 Hz), 7.77 (2H, d, $J$ = 8.7 Hz); MS *m/z* 400 $(M + H)^+$.

A mixture of the ester (1.00 g, 2.51 mmol) obtained above and 20 wt % aqueous NaOH (1.50 g) in acetone (4 mL) was stirred at 50 °C for 1 h before dilution with water (12 mL). The product that was precipitated by acidification to pH 1 with 6 M HCl was collected by filtration and washed with water (2 × 5 mL) to afford **9** (0.91 g, 94%) as a white crystalline solid, mp 107−108 °C: $^1$H NMR (400 MHz, $CDCl_3$) $\delta$ 1.04 (6H, d, $J$ = 6.6 Hz), 1.07 (3H, t, $J$ = 7.4 Hz), 1.80−1.94 (2H, m), 2.04−2.20 (1H, m), 2.71, 2.99 (each 2H, t, $J$ = 7.6 Hz), 3.79 (2H, d, $J$ = 6.6 Hz), 4.01 (2H, t, $J$ = 6.5 Hz), 6.88 (1H, d, $J$ = 8.3 Hz), 6.95 (2H, d, $J$ = 8.7 Hz), 7.66 (1H, d, $J$ = 2.1 Hz), 7.69 (1H, dd, $J$ = 8.3, 2.1 Hz), 7.76 (2H, d, $J$ = 8.7 Hz); MS *m/z* 383 $(M - H)^-$. Anal. ($C_{23}H_{28}O_5$) C, H.

**3-[2-Benzyloxy-5-(4-isobutoxybenzoyl)phenyl]propionic Acid (11).** Compound **28** was treated by the procedure described for **9** except using benzyl bromide to afford **11** (67%) as a white solid, which was crystallized from hexane/diisopropyl ether to give colorless crystals, mp 100 °C: $^1$H NMR (400 MHz, $CDCl_3$) $\delta$ 1.04 (6H, d, $J$ = 6.6 Hz), 2.02−2.18 (1H, m), 2.72 (2H, t, $J$ = 7.6 Hz), 3.04 (2H, t, $J$ = 7.6 Hz), 3.79 (2H, d, $J$ = 6.6 Hz), 5.17 (2H, s), 6.91−6.98 (3H, m), 7.30−7.48 (5H, m), 7.64−7.70 (2H, m), 7.76 (2H, d, $J$ = 8.8 Hz); MS *m/z* 431 $(M - H)^-$. Anal. ($C_{27}H_{28}O_5$) C, H.

**3-[2-Isobutoxy-5-(4-propoxybenzoyl)phenyl]propionic Acid (10).** Compound **29** was treated by the procedure described for **9** except using isobutyl bromide to afford **10** (85%) as a white crystalline solid, mp 128−129 °C: $^1$H NMR (400 MHz, $CDCl_3$) $\delta$ 1.00−1.12 (9H, m), 1.76−1.92 (2H, m), 2.08−2.24 (1H, m), 2.71 (2H, t, $J$ = 7.6 Hz), 3.00 (2H, t, $J$ = 7.6 Hz), 3.82 (2H, d, $J$ = 6.4 Hz), 4.00 (2H, t, $J$ = 6.6 Hz), 6.87 (1H, d, $J$ = 8.4 Hz), 6.95 (2H, d, $J$ = 8.7 Hz), 7.66 (1H, d, $J$ = 2.1 Hz), 7.69 (1H, dd, $J$ = 8.4, 2.1 Hz), 7.76 (2H, d, $J$ = 8.7 Hz); MS *m/z* 383 $(M - H)^-$. Anal. ($C_{23}H_{28}O_5$) C, H.

**3-[5-(4-Benzyloxybenzoyl)-2-isobutoxyphenyl]propionic Acid (12).** Compound **30** was treated by the procedure described for **9** except using isobutyl bromide to afford **12** (79%) as a white solid, which was crystallized from $CH_2Cl_2$/hexane to give colorless crystals, mp 150−151 °C: $^1$H NMR (400 MHz, $CDCl_3$) $\delta$ 1.06 (6H, d, $J$ = 6.6 Hz), 2.08−2.20 (1H, m), 2.71 (2H, t, $J$ = 7.7 Hz), 3.00 (2H, t, $J$ = 7.7 Hz), 3.82 (2H, d, $J$ = 6.3 Hz), 5.15 (2H, s), 6.87 (1H, d, $J$ = 8.3 Hz), 7.03 (2H, d, $J$ = 8.7 Hz), 7.30−7.48 (5H, m), 7.60−7.72 (2H, m), 7.77 (2H, d, $J$ = 8.7 Hz); MS *m/z* 432 $(M - H)^-$. Anal. ($C_{27}H_{28}O_5$) C, H.

**Bis(4-isobutoxyphenyl)methanone (8).** To a stirred suspension of bis(4-hydroxyphenyl)methanone (2.00 g, 9.34 mmol) and $K_2CO_3$ (3.87 g, 28.0 mmol) in DMF (20 mL) at room temperature was added isobutyl bromide (3.84 g, 28.0 mmol), and then the mixture was heated with stirring at 100 °C for 1 h. Additional $K_2CO_3$ (1.29 g, 9.33 mmol) and isobutyl bromide (1.28 g, 9.34 mmol) were then added, and the heating was continued for a further 1.5 h. The reaction mixture was cooled to room temperature before filtration, and the residue was rinsed with EtOAc (3 × 30 mL). The filtrate was treated with water (50 mL) followed by acidification to pH 2 with 6 M HCl, and the aqueous layer separated was extracted with EtOAc (1 × 30 mL). The combined organic extracts were washed with water (1 × 30 mL) and brine (1 × 30 mL), followed by the addition of $CHCl_3$ (30 mL). The solution was dried over $MgSO_4$ and concentrated under reduced pressure. The residue was triturated with hexane (20 mL) to afford **8** (2.88 g, 94%) as a white solid, which was crystallized from $CH_2Cl_2$/hexane to give colorless crystals, mp 118−119 °C: $^1$H NMR (400 MHz, $CDCl_3$) $\delta$ 1.05 (12H, d, $J$ = 6.8 Hz), 2.04−2.20 (2H, m), 3.80 (4H, d, $J$ = 6.6 Hz), 6.95 (4H, d, $J$ = 8.5 Hz), 7.77 (4H, d, $J$ = 8.5 Hz); MS *m/z* 327 $(M + H)^+$. Anal. ($C_{21}H_{26}O_3$) C, H.

**3-[2-Isobutoxy-5-(4-isobutoxybenzoyl)phenyl]propionamide (13).** To a stirred solution of **4** (5.00 g, 12.5 mmol) in THF (50 mL) at room temperature was sequentially added oxalyl chloride (1.91 g, 15.0 mmol) and DMF (50 $\mu$L), and the mixture was stirred for 3 h. The resulting mixture was slowly poured into ice-cooled 25 wt % $NH_4OH$ (50 mL) with vigorous stirring. After being stirred at 5 °C for 30 min, the mixture was adjusted to pH 6 with 6 M HCl and extracted with EtOAc (1 × 100 mL). The aqueous layer separated was extracted with EtOAc (1 × 50 mL), and the organic extracts were washed with water (1 × 50 mL) and brine (1 × 50 mL), dried over $MgSO_4$, and concentrated under reduced pressure. The residual solid was triturated with hexane (100 mL) to afford **13** (4.67 g, 94%) as a white solid, which was crystallized from $CH_2Cl_2$/hexane to give colorless crystals, mp 123 °C: $^1$H NMR (400 MHz, $CDCl_3$) $\delta$ 1.05 (6H, d, $J$ = 6.8 Hz), 1.08 (6H, d, $J$ = 6.6 Hz), 2.06−2.22 (2H, m), 2.56 (2H, t, $J$ = 7.7 Hz), 3.02 (2H, t, $J$ = 7.7 Hz), 3.80 (2H, d, $J$ = 6.6 Hz), 3.83 (2H, d, $J$ = 6.3 Hz), 5.29 (1H, br s), 5.38 (1H, br s), 6.88 (1H, d, $J$ = 8.1 Hz), 6.95 (2H, d, $J$ = 8.5 Hz), 7.62−7.70 (2H, m), 7.76 (2H, d, $J$ = 8.5 Hz); MS *m/z* 399 $(M + H)^+$. Anal. ($C_{24}H_{31}NO_4$) C, H, N.

**ELISA-Based AP-1 Binding Assay: Preparation of c-Fos and c-Jun bZIP Peptides.** The resin and all of the protected amino acids and coupling reagents were purchased from Watanabe Chemical Industries (Hiroshima, Japan). All of the reagents and solvents were reagent grade or better and were used without further purification. High-performance liquid chromatography (HPLC) was performed using a Hitachi L-7100 apparatus equipped with an L-7400 UV detector (peak detection at 230 nm) and a PROTEINE-RP column (YMC−Pack, YMC Co., Kyoto, Japan) of 250 × 20 mm for preparative HPLC or 150 × 4.6 mm for analytical HPLC. c-Jun bZIP peptide [c-Jun (263−324) Cys278Ser] and biotinylated c-Fos bZIP peptide [*N*-biotinyl-(Gly)$_4$-c-Fos (139−200) Cys154Ser][5] were synthesized manually using standard solid-phase peptide chemistry with *tert*-butoxycarbonyl (Boc)-protected amino acids on Boc-His(benzyloxymethyl)-PAM resin[24] at a 0.30 mmol scale. The Boc protecting group was removed by treatment with trifluoroacetic acid (10 mL) at room temperature for 3 min. Coupling with Boc-protected amino acids (4 equiv) was then performed in the presence of *N,N*-diisopropylethylamine (6 equiv) and 2-(1*H*-benzotriazol-1-yl)-1,1,3,3-tetramethyluronium hexafluorophosphate (3.8 equiv) in *N*-methyl-2-pyrrolidone (8 mL) at room temperature for 30 min.[25] Subsequently, the peptide resin was treated with decanoic anhydride (0.3 mol/L in 1:1 DMF/$CH_2Cl_2$, 10 mL) at room temperature for 30 min. The protected c-Jun bZIP peptide resin (0.50 g) was treated with a reagent containing anhydrous HF (1.5 mL) and dimethyl sulfide (4.5 mL) with stirring at 0 °C for 1.5 h to remove the remaining O- and N-protecting groups.[26] After the evaporation of HF, ether was added to the resin, which was then filtered, washed in $CH_2Cl_2$ (5 × 10 mL), followed by dried in vacuo. The resin was treated with a reagent containing anhydrous HF (4.5 mL) and *p*-cresol (1.5 mL) with stirring at 0 °C for 1.5 h to induce cleavage of the peptide from the resin. The precipitate was collected by centrifugation and dissolved in water. The exhausted resin was filtered, and the filtrate was purified by reverse phase HPLC eluted with a linear gradient of acetonitrile in water containing 0.1% trifluoroacetic acid at a flow rate of 7.0 mL/min before lyophilization. Biotinylated c-Fos bZIP peptide was synthesized according to the procedure that was used to prepare the c-Jun bZIP peptide.

The peptides were separately dissolved in 20 mM Tris-HCl buffer (pH 7.5) containing 50 mM KCl, 1 mM ethylenediaminetetraacetic acid (EDTA), 10 mM $MgCl_2$, 1 mM dithiothreitol (DTT), 0.5 M

guanidine HCl, and 30% glycerol. Equimolar quantities of both of the solutions were mixed together and the resulting mixture was used as the AP-1 bZIP peptide.

**Binding Assay of AP-1 bZIP Peptide and AP-1 Double-Stranded Oligonucleotides.** The inhibitory activities of the synthetic compounds on the DNA-binding activity of AP-1 were evaluated using an ELISA-based AP-1 binding assay with synthetic double-stranded oligonucleotides that contained the AP-1 binding site (shown in bold) and the AP-1 bZIP peptide. The AP-1 bZIP peptide (10 pmol/well) was added to an avidin-coated 96-well ELISA plate, washed, and then blocked with bovine serum albumin. Digoxigenin-labeled double-stranded oligonucleotides (22-mer) containing an AP-1 binding sequence (5′-CTAGTGATGAGTCAGCCGGATC-3′ and 5′-GATCCGGCTGACTCATCACTAG-3′) (Nisshinbo Industries, Inc., Tokyo, Japan) were reacted in the presence or absence of each sample at room temperature for 1 h in a binding reaction solution [25 mM Tris-HCl (pH 7.9) containing 0.5 mM EDTA, 0.05% Nonidet P-40 and 10% glycerol]. Subsequently, the unbound labeled oligonucleotide was washed out with HEPES−KOH (pH 7.9) buffer containing 0.5 mM EDTA, 50 mM KCl, 10% glycerol, 0.1% BSA, and 0.05% Tween-20. The peroxidase-conjugated anti-digoxigenin antibody (Roche Diagnostics, Indianapolis, IN) was then added and reacted with the labeled oligonucleotide bound to AP-1. After washing out the excess antibody with HEPES−KOH buffer containing 0.05% Tween-20, the residue was reacted for a predetermined period of time in 100 mM citrate buffer (pH 5.0) containing 0.03% $H_2O_2$ using *o*-phenylenediamine as a substrate. After adding sulfuric acid solution to each well, the absorbance at 492 nm was measured with a Microplate spectrophotometer (Bio-Rad Laboratories, Hercules, CA). Taking the absorbance in the absence of sample as 100%, the inhibition rate of each sample was calculated from the absorbance in the presence of the sample. The $IC_{50}$ values were calculated based on a logistic concentration−response curve using the SAS system version 8.2 (SAS Institute, Cary, NC).

**Cell-Based Assay: Plasmids.** Reporter plasmids containing the firefly luciferase reporter gene driven by a basic promoter element (TATA box) plus a defined inducible cis-enhancer element were utilized (PathDetect in Vivo Signal Transduction Pathway *cis*-Reporting Systems, Stratagene, La Jolla, CA). The firefly luciferase gene in the reporter plasmid (pAP-1-Luc) was controlled by synthetic enhancer sequences comprising seven repeats of the binding sites for AP-1; TGACTAA. A control plasmid expressing *Renilla reniformis* luciferase driven by the herpes simplex virus thymidine kinase promoter, phRL-TK Vector (Promega, Madison, WI), was used to correct the efficiency of transfection.

**Cell Culture.** The murine fibroblast cell line NIH3T3 was obtained from the American Type Culture Collection (ATCC No. CRL-1658; Rockville, MD) and grown in Dulbecco's modified Eagle's medium (DMEM; Nissui Pharmaceutical, Tokyo, Japan) supplemented with 4 mM l-glutamine (Wako Pure Chemical, Osaka, Japan), 1.5 g/L glucose (Wako Pure Chemical), 10% heat-inactivated fetal calf serum (FCS; JRH Biosciences, Lenexa, KS), and 60 μg/mL kanamycin sulfate (Sigma-Aldrich, St. Luis, MO) at 37 °C and 5% $CO_2$.

**Transient Transfection and Reporter Gene Assay.** Approximately $1 \times 10^4$ cells in 100 μL of 10% FCS-DMEM were plated into a 96-well tissue culture plate (Iwaki Glass, Chiba, Japan) 24 h before transfection (day 0). On day 1, the cells in each well were transiently cotransfected with 40 ng of pAP-1-Luc plasmid and 4 ng of phRL-TK Vector using the FuGENE 6 transfection reagent (Roche Diagnostics, Indianapolis, IN). After transfection for 6 h at 37 °C, the cells were cultured in 0.5% FCS-DMEM. On day 2, the medium was exchanged with 0.5% FCS-DMEM containing the compounds. After 1 h, phorbol 12-myristate 13-acetate (TPA) was added to each well (100 ng/mL). Three hours after TPA stimulation, whole cell lysates were examined for luciferase activity (Dual-Luciferase Reporter Assay System, Promega) with a luminometer (Luminous CT-9000D; DIA-IATRON, Tokyo, Japan) according to the manufacturer's protocol. The firefly luciferase activity was normalized for transfection efficiency based on the Renilla luciferase activity. Taking the activity in the absence of sample as 100%, the inhibition rate of each sample was calculated from the absorbance in the presence of the sample. The $IC_{50}$ values were calculated based on a logistic concentration−response curve using the SAS system version 8.2.

**Acknowledgment.** This study was partially supported by the Japan Science and Technology Agency.

**Supporting Information Available:** Characterization data for esters of compounds **5**−**7** and **10**−**12** plus elemental analysis data for compounds **2**−**13**. This material is available free of charge via the Internet at http://pubs.acs.org.

## References

(1) Angel, P.; Karin, M. The Role of Jun, Fos and the AP-1 Complex in Cell-Proliferation and Transformation. *Biochim. Biophys. Acta* **1991**, *1072*, 129−157.
(2) Wagner, E. F. AP-1 − Introductory Remarks. *Oncogene* **2001**, *20*, 2334−2335.
(3) Shiozawa, S.; Shimizu, K.; Tanaka, K.; Hino, K. Studies on the Contribution of c-fos/AP-1 to Arthritic Joint Destruction. *J. Clin. Invest.* **1997**, *99*, 1210−1216.
(4) Suto, M. J.; Ransone, L. J. Novel Approaches for the Treatment of Inflammatory Diseases: Inhibitors of NF-κB and AP-1. *Curr. Pharm. Des.* **1997**, *3*, 515−528.
(5) Glover, J. N. M.; Harrison, S. C. Crystal Structure of the Heterodimeric bZIP Transcription Factor c-Fos-c-Jun Bound to DNA. *Nature* **1995**, *373*, 257−261.
(6) Hahm, E.-R.; Cheon, G.; Lee, J.; Kim, B.; Park, C.; Yang, C.-H. New and Known Symmetrical Curcumin Derivatives Inhibit the Formation of Fos-Jun-DNA Complex. *Cancer Lett.* **2002**, *184*, 89−96.
(7) Park, S.; Lee, D.-K.; Yang, C.-H. Inhibition of Fos-Jun-DNA Complex Formation by Dihydroguaiaretic Acid and In Vitro Cytotoxic Effects on Cancer Cells. *Cancer Lett.* **1998**, *127*, 23−28.
(8) Goto, M.; Masegi, M.; Yamauchi, T.; Chiba, K.; Kuboi, Y.; Harada, K.; Naruse, N. K1115 A, a New Anthraquinone Derivative that Inhibits the Binding of Activator Protein-1 (AP-1) to its Recognition Sites. *J. Antibiot.* **1998**, *51*, 539−544.
(9) Tsuchida, K.; Chaki, H.; Takakura, T.; Yokotani, J.; Aikawa, Y.; Shiozawa, S.; Gouda, H.; Hirono, S. Design, Synthesis, and Biological Evaluation of New Cyclic Disulfide Decapeptides That Inhibit the Binding of AP-1 to DNA. *J. Med. Chem.* **2004**, *47*, 4239−4246.
(10) Olson, G. L.; Bolin, D. R.; Bonner, M. P.; Bös, M.; Cook, C. M.; Fry, D. C.; Graves, B. J.; Hatada, M.; Hill, D. E.; Kahn, M.; Madison, V. S.; Rusiecki, V. K.; Sarabu, R.; Sepinwall, J.; Vincent, G. P.; Voss, M. E. Concepts and Progress in the Development of Peptide Mimetics. *J. Med. Chem.* **1993**, *36*, 3039−3049.
(11) Gante, J. Peptidomimetics−Tailored Enzyme Inhibitors. *Angew. Chem., Int. Ed. Engl.* **1994**, *33*, 1699−1720.
(12) Hruby, V. J.; Balse, P. M. Conformational and Topographical Considerations in Designing Agonist Peptidomimetics from Peptide Leads. *Curr. Med. Chem.* **2000**, *7*, 945−970.
(13) Cramer, R. D.; Jilek, R. J.; Guessregen, S.; Clark, S. J.; Wendt, B.; Clark, R. D. "Lead Hopping". Validation of Topomer Similarity as a Superior Predictor of Similar Biological Activities. *J. Med. Chem.* **2004**, *47*, 6777−6791.
(14) Schneider, G.; Böhm, H.-J. Virtual Screening and Fast Automated Docking Methods. *Drug Discovery Today* **2002**, *7*, 64−70.
(15) Honma, T.; Hayashi, K.; Aoyama, T.; Hashimoto N.; Machida T.; Fukasawa K.; Iwama T.; Ikeura C.; Ikuta M.; Suzuki-Takahashi I.; Iwasawa Y.; Hayama T.; Nishimura S.; Morishima H. Structure-Based Generation of a New Class of Potent Cdk4 Inhibitors: New de Novo Design Strategy and Library Design. *J. Med. Chem.* **2001**, *44*, 4615−4627.
(16) Schneider, G.; Fechner, U. Computer-Based *De Novo* Design of Drug-Like Molecules. *Nat. Rev. Drug Discovery* **2005**, *4*, 649−663.
(17) Nyburg, S. C. Some Uses of a Best Molecular Fit Routine. *Acta Crystallogr.* **1974**, *B30* (part I), 251−253.
(18) Oya, M.; Baba, T.; Kato, E.; Kawashima, Y.; Watanabe, T. Synthesis and Antihypertensive Activity of *N*-(Mercaptoacyl)-thiazolidinecarboxylic Acids. *Chem. Pharm. Bull.* **1982**, *30*, 440−461.
(19) Smith, R. A. Studies in the Rearrangements of Phenyl Ethers. The Action of Aluminum Chloride on Butyl Phenyl Ethers. *J. Am. Chem. Soc.* **1933**, *55*, 3718−3721.

(20) Schuda, P. F.; Price, W. A. Total Synthesis of Isoflavones: Jamaicin, Calopogonium Isoflavone-B, Pseudobaptigenin, and Maxima Substance-B. Friedel–Crafts Acylation Reactions with Acid-Sensitive Substrates. *J. Org. Chem.* **1987**, *52*, 1972–1979.
(21) Dalcanale, E.; Montanari, F. Selective Oxidation of Aldehydes to Carboxylic Acids with Sodium Chlorite-Hydrogen Peroxide. *J. Org. Chem.* **1986**, *51*, 567–569.
(22) *SYBYL 6.5*; Tripos, Inc.: St. Louis, MO, 1998.
(23) Halgren, T. A. Merck Molecular Force Field. I. Basis, Form, Scope, Parameterization, and Performance of MMFF94. *J. Comput. Chem.* **1996**, *17*, 490–519.
(24) Mitchell, A. R.; Erickson, B. W.; Ryabtsev, M. N.; Hodges, R. S.; Merrifield, R. B. *tert*-Butoxycarbonylaminoacyl-4-(oxymethyl)-phenylacetamidomethyl-Resin, a More Acid-Resistant Support for Solid-Phase Peptide Synthesis. *J. Am. Chem. Soc.* **1976**, *98*, 7357–7362.
(25) Knorr, R.; Trzeciak, A.; Bannwarth, W.; Gillessen, D. New Coupling Reagents in Peptide Chemistry. *Tetrahedron Lett.* **1989**, *30*, 1927–1930.
(26) Tam, J. P.; Heath, W. F.; Merrifield, R. B. $S_N2$ Deprotection of Synthetic Peptides with a Low Concentration of HF in Dimethyl Sulfide: Evidence and Application in Peptide Synthesis. *J. Am. Chem. Soc.* **1983**, *105*, 6442–6455.

JM050550D